



Universiteit
Leiden
The Netherlands

Antigen handling and cross-presentation by dendritic cells

Ho, N.I.S.C.

Citation

Ho, N. I. S. C. (2020, July 9). *Antigen handling and cross-presentation by dendritic cells*. Retrieved from <https://hdl.handle.net/1887/123272>

Version: Publisher's Version

License: [Licence agreement concerning inclusion of doctoral thesis in the Institutional Repository of the University of Leiden](#)

Downloaded from: <https://hdl.handle.net/1887/123272>

Note: To cite this publication please use the final published version (if applicable).

Cover Page



Universiteit Leiden



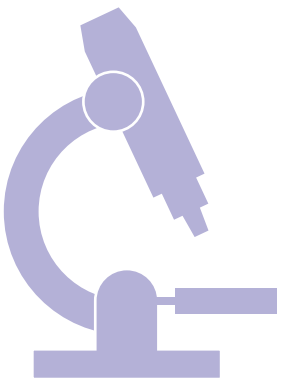
The handle <http://hdl.handle.net/1887/123272> holds various files of this Leiden University dissertation.

Author: Ho, N.I.S.C.

Title: Antigen handling and cross-presentation by dendritic cells

Issue Date: 2020-07-09

5



Glycan modification of antigen alters its intracellular routing in dendritic cells, promoting priming of T cells

Ingeborg Streng-Ouwehand, Nataschja I. Ho, Manja Litjens, Hakan Kalay, Martine A. Boks, Lenneke A.M Cornelissen, Satwinder Kaur Singh, Eirikur Saeland, Juan J. García-Vallejo, Ferry Ossendorp, Wendy W.J. Unger, Yvette van Kooyk

Elife 2016 Mar 21; 5. pii: e11765



ABSTRACT

Antigen uptake by dendritic cells and intracellular routing of antigens to specific compartments is regulated by C-type lectin receptors that recognize glycan structures. We show that modification of Ovalbumin (OVA) with the glycan-structure Lewis^x (Le^x) re-directs OVA to the C-type lectin receptor MGL1. Le^x-modification of OVA favored Th1 skewing of CD4⁺ T cells and enhanced cross-priming of CD8⁺ T cells. While cross-presentation of native OVA requires high antigen dose and TLR stimuli, Le^x modification reduces the required amount 100-fold and obviates its dependence on TLR signaling. The OVA-Le^x induced enhancement of T cell cross-priming is MGL1-dependent as shown by reduced CD8⁺ effector T cell frequencies in MGL1-deficient mice. Moreover, MGL1-mediated cross-presentation of OVA-Le^x neither required TAP-transporters nor cathepsin S and was still observed after prolonged intracellular storage of antigen in Rab11⁺LAMP1⁺ compartments. We conclude that controlled neo-glycosylation of antigens can crucially influence intracellular routing of antigens, the nature and strength of immune responses and should be considered for optimizing current vaccination strategies.

INTRODUCTION

The induction of T cell immunity to viruses or tumors involves the presentation of viral or tumor antigens by antigen-presenting cells (APC) in the context of major histocompatibility complex (MHC) molecules. Loading of exogenously-derived antigens onto MHC class I molecules, a process known as cross-presentation (1) is required to activate antigen-specific CD8⁺ T cells. Furthermore, cognate CD4⁺ T cell help is important for licensing the APC, which is essential for effective CD8⁺ T cell priming and induction of long-lasting memory (2, 3). The molecular mechanisms underlying cross-presentation have been studied intensively, however, little is still known on the nature of the antigens and stimuli that are required for APC to route exogenous antigens efficiently into the MHC class I presentation pathway. Most exogenous antigens that originate from tumor cells or viruses are glycosylated in their native form (4). The relative composition of the glycosylation machinery, which includes all the necessary glycosylation-related enzymes and co-factors, determines the final configuration of the glycan structures that decorate *N*- or *O*-linked glycosylation sites present in glycoproteins. The glycosylation machinery can be affected by multiple physio-pathological cues, including proliferation, activation, and the transformation status of the cell (5), and depends on environmental factors. APC, such as dendritic cells (DCs) and macrophages are able to sense glycans exposed on either self- or pathogen-derived antigens via glycan-binding proteins. Amongst these glycan-binding proteins are C-type lectin receptors (CLRs) that recognize defined carbohydrate-structures through their carbohydrate recognition domain (CRD). Depending on the amino acid sequence, the CRD bears specificity for mannose, fucose, galactose, sialylated-, or sulfated structures. CLRs function both as antigen uptake and/or signaling receptors that modify DC-induced cytokine responses thereby influencing T cell differentiation (6). The specialized internalization motifs in the cytoplasmic domains of CLRs allow the rapid internalization of antigens upon interaction (7, 8). This suggests that DCs use CLRs to “sense” the natural glycan composition of tissues and invading pathogens and, in response to this recognition, are able to modulate immune responses (9).

The conjugation of antigens to CLRs-specific antibodies, such as DEC205, mannose receptor (MR), Dendritic Cell-Specific Intercellular adhesion molecule-3-Grabbing Non-integrin (DC-SIGN) or CLEC9A, has proven to be an effective way to direct antigens to DCs, resulting in enhanced antigen uptake and presentation on MHC molecules (10–13). Also glycans specific for CLRs have shown their targeting specificity and potential to improve antigen uptake and presentation in MHC class I and II molecules when coupled to antigen formulations (14–20). To achieve immunity rather than tolerance inclusion of a strong adjuvant is necessary. Little is known on how naturally glycosylated antigens or alterations

in the glycosylation of antigens may change and re-direct antigen internalization via CLRs, in addition to subsequent processing and presentation.

MR was shown to mediate cross-presentation of the model-antigen ovalbumin (OVA) in a Toll-like receptor (TLR)-dependent manner and to recruit TAP-1 to endocytic organelles (21, 22). Importantly, cross-presentation of OVA was only effective using high amounts of antigen (21, 22). The interaction of OVA with MR, which has specificity for mannose (23), was speculated to be dependent on the presence of mannose glycans on OVA (22). In the current study, we investigated the effect of modifying the glycan composition of OVA on the efficacy of cross-presentation, priming and differentiation of T cells. We hypothesized that modification of the antigen with specific glycans would re-direct antigens to other CLRs resulting in altered intracellular routing and presentation of antigen and Th differentiation. We have chosen to conjugate the carbohydrate structure Lewis^x (Le^x) to 2 free cysteine residues within the native OVA glycoprotein. Le^x is a ligand of the murine C-type lectin macrophage galactose-type lectin (MGL)-1 (24), which is expressed on murine plasmacytoid DCs, CD8⁺ and CD8⁻ splenic DCs, DCs in the small intestines, the sub-capsular and intra-follicular sinuses of T cell areas in lymph nodes, and on DCs and macrophages in the dermis of skin (25–28). Murine MGL1 is one of two homologues (MGL1 and MGL2) of human MGL (huMGL), which has been shown to interact with tumor cells through glycans exposed on MUC1 as well as with various pathogens (29). However, MGL1 and MGL2 bind different glycan structures: while MGL1 binds Le^x and Le^a glycans, MGL2 binds *N*-acetylgalactosamine (GalNAc) and galactose glycan structures (24). The YENF motif in the cytoplasmic tail of huMGL is essential for uptake of soluble antigens, which are subsequently presented to CD4⁺ T cells (30). Murine MGL1 contains a similar motif (YENL) in its cytoplasmic tail, which likely plays a similar and important role in antigen uptake (31). Glycan binding to the CLRs DC-SIGN, Dectin-1 and Dectin-2 has been demonstrated to trigger the signaling capacity of these receptors, modulating DC-mediated T helper cell (Th) differentiation and cytokine production by DCs (9). This illustrates that glycan epitopes may not only improve antigen presentation, but may also affect Th differentiation and shape specific adaptive immune responses. This is underlined by the observation that DC-SIGN signaling induced upon sensing of specific mannose or fucose structures on pathogens differentially directed Th differentiation (32).

Here, we demonstrate that conjugation of the Le^x carbohydrate to the model antigen OVA alters its routing from a MR- and TAP-1-dependent cross-presentation pathway into a TAP-1- and cathepsin S-independent pathway, devoid of any TLR-signaling dependence, which simultaneously enhanced CD8⁺ T cell priming and Th1 skewing of CD4⁺ T cells. Cross-presentation was associated with prolonged intracellular storage of antigen in Rab11⁺LAMP1⁺ vesicles. Our results illustrate that small changes in the glycosylation profile of protein antigens can have a great impact on antigen routing within DCs, affecting cross-presentation and Th cell differentiation.

RESULTS

Identification of glycans on native and glycan-modified OVA, and the consequences for CLR-specific binding and cross-presentation

The well-known model antigen OVA carries one *N*-glycosylation site at N293 and, although the variety of OVA glycans have been previously described, their relative abundance has never been characterized in detail. We determined the glycan profile of OVA by normal-phase HPLC coupled to electrospray ionization mass spectrometry with an intercalated fluorescence detector. We found that the majority of glycan species on OVA corresponded to the complex-type (54.9%), while mannose-rich glycans (mainly Man5 and Man6, potential ligands of the MR (33) represented only 23% of all glycoforms (Figure 1A). The remaining glycoforms were of the hybrid (16.2%) and oligomannose (Man3, 3%) type. The presence of mannose rich glycans on OVA correlate with the earlier reports that in particular MR interacted with OVA (34) and mediated the TLR dependent and TAP-1 dependent cross-presentation of OVA (21). We reasoned that the conjugation of additional glycans to OVA would alter its CLR-dependent effects. To do this, we conjugated the tri-saccharide glycan structure Le^x (Galβ1-4(Fuca1-3)GlcNAc) to the free cysteins of OVA using standard thiol-maleimide chemistry via the bifunctional crosslinker MPBH. Le^x is a well characterized carbohydrate ligand of the C-type lectin MGL1 (11, 24). Using mass spectrometry (MALDI-TOF/TOF), we confirmed that OVA-Le^x increases to 1.2 KDa in mass, indicating that at least 40 % of the total OVA-Le^x preparation contained the Le^x (Figure 1-figure supplement 1). This increase corresponded to the addition of two Le^x molecules per OVA molecule. Furthermore, using anti-Le^x antibodies the presence of Le^x was detected on OVA-Le^x, whereas absent on native glycosylated OVA, indicating that the glycan was successfully conjugated to OVA (Figure 1B). While native OVA interacted with the MR (MR-Fc, Figure 1B) and as earlier described (22), the conjugation of Le^x to OVA conferred high-avidity binding to MGL1 as revealed using the soluble recombinant form of MGL1 (MGL1-Fc, Figure 1B). Moreover, the addition of Le^x to OVA did not result in increased binding to the MR binding, indicating that Le^x selectively binds MGL1. Similar binding with an anti-OVA antibody was determined, which indicates that similar protein concentrations in the preparations of OVA and OVA-Le^x used in our study are present (Figure 1B, right panel). In conclusion, through glycan profiling we identified 23% mannose-rich glycans on native OVA that may facilitate MR binding. Addition of the glycan Le^x, next to these mannose glycans, on cysteine residues (two Le^x moieties per molecule), conveyed MGL1 specificity to OVA.

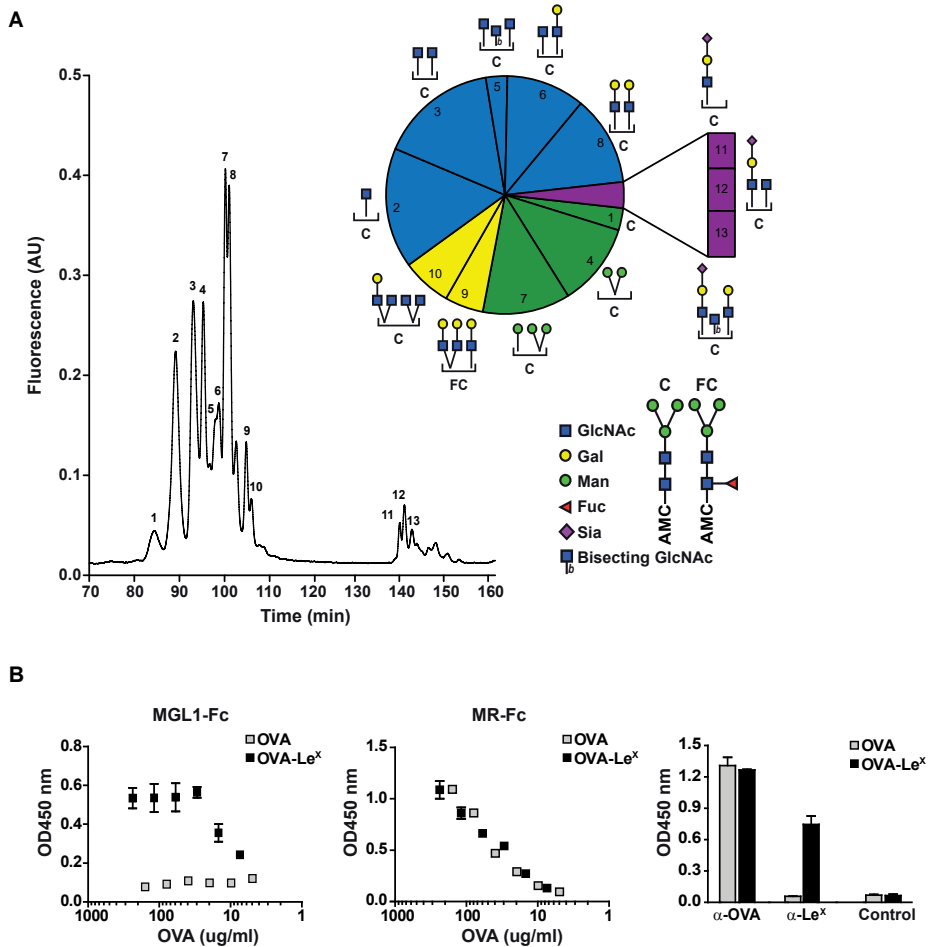


Figure 1. Generation of OVA-neo-glycoconjugates with Le^x that confers binding of OVA to MGL1. (A) A glycan profile of OVA was generated using a multidimensional normal phase nano-HPLC coupled to an electrospray ionization interface mass spectrometer with an intercalated nano fluorescence detector. The different glycan species, indicated by numbers, are shown on the right; their relative proportion is represented in a pie chart. (B) ELISA showing functional modification of OVA with Le^x glycans, as detected with anti-Le^x antibodies and resulting in binding of MGL1-Fc. Unconjugated OVA does not carry any ligands for MGL1. Modification of OVA with Le^x did not alter the ability to bind to MR as illustrated by equal binding kinetics of MR-Fc to native OVA and OVA-Le^x. OVA and OVA-Le^x preparations contain similar amounts of OVA as detected with anti-OVA antibodies.

OVA-Le^x binds MGL1 and augments priming of OVA-specific CD8⁺ T cells in-vivo

We explored the potency of OVA-Le^x to enhance T cell priming *in vivo*. Since DCs are crucial for priming of naive T cells, we first established the presence of MGL on both splenic and bone marrow-derived DCs (spDCs and BM-DCs) of C57BL/6 mice by staining with the anti-

MGL antibody ER-MP23 (Figure 2A). Since the ER-MP23 antibody does not discriminate between the two murine MGL homologues MGL1 and MGL2, MGL1 expression in wild type (WT) CD11c⁺ DCs was confirmed using qRT-PCR (Figure 2B). Immunization of mice with OVA-Le^x mixed with agonistic anti-CD40 antibodies resulted in the enhanced priming of OVA-specific CD8⁺ T cells as revealed from both higher numbers of OVA/H-2K^b tetramer binding CD8⁺ T cells and OVA-specific IFN- γ and TNF-producing CD8⁺ T cells than obtained with native OVA (Figure 2C, Figure 2-figure supplement 1). Using MGL1 KO mice, that lack MGL1 expression on DCs (Figure 2B), we ascertained that MGL1 is the prime lectin involved in boosting the generation of antigen-specific effector T cells as upon immunization of these mice with Le^x-conjugated OVA no enhanced frequencies of OVA-specific IFN- γ and TNF α -double-producing T cells were detected (Figure 2D, Figure 2-figure supplement 2). In fact, the OVA-Le^x immunized MGL1 KO mice displayed comparable numbers of effector T cells as WT mice immunized with native OVA. Together, these data show that the conjugation of two Le^x glycans on OVA re-directs OVA to the CLR MGL1 and thereby enhances CD8⁺ T cell priming *in vivo*.

OVA-Le^x induces Th1 skewing of naive CD4⁺ T cells

Since we observed that Le^x-modified OVA increased priming of antigen-specific CD8⁺ T cells we examined whether this also enhanced antigen-presentation to CD4⁺ T cells. Both OVA-Le^x-loaded and native OVA-loaded spDCs induced CD4⁺ OT-II T cell proliferation to a similar extent (Figure 3A), illustrating that the altered antigen uptake mediated by Le^x did not affect loading on MHC class II molecules. Similar results were obtained using BM-DCs (Figure 3A). Although we did not observe any differential effect of Le^x on CD4⁺ T cell expansion, neoglycosylation of antigens could induce signaling via CLRs and herewith potentially influence Th cell differentiation (32). We therefore investigated whether OVA-Le^x affected the differentiation of naive CD4⁺ T cells. Hereto BM-DCs and spDCs of C57BL/6 mice were pulsed with OVA-Le^x and subsequently co-cultured with naive CD4⁺CD62L^{hi} OT-II cells. Co-cultures containing OVA-Le^x loaded BM-DCs or spDCs contained significantly more IFN- γ -producing T cells than those containing OVA-loaded DCs (Figure 3B). Neither induction of IL-4- nor IL-17A-producing CD4⁺ T cells was observed (Figure 3B, upper and middle panel and data not shown). In addition, induction of Foxp3⁺ T cells was not detected (data not shown). To exclude that the Th1 skewing by OVA-Le^x loaded DCs was attributed to the more Th1 prone status of C57BL/6 (35), we also performed the Th-differentiation assay with cells derived from Th2 prone BALB/c mice (36). We observed that naive OVA-specific CD4⁺ T cells from DO11.10 Tg mice that were stimulated with OVA-loaded BM-DCs differentiated into IL-4 secreting T cells (Figure 3B, lower panels). However, the generation of IL-4-producing T cells was not influenced by loading DCs with OVA-Le^x as these cultures contained comparable percentages of IL-4-producing DO11.10 T cells. Using these Th2-prone T cells, OVA-Le^x-pulsed

DCs still induced considerably more IFN- γ -producing CD4⁺ T cells than native OVA-pulsed DCs (Figure 3B, lower panel). Since this assay takes three days longer than the antigen-presentation assay, it is possible that the higher frequency of IFN- γ -producing CD4⁺ T cells is due to increased division of OVA-specific CD4⁺ T cells. However, we found that the amount of proliferation of OVA-specific CD4⁺ T cells induced by stimulation with OVA-Le^x-loaded DCs after 6 days is similar to that induced by OVA-loaded DCs (Figure 3-figure supplement 1). The augmented induction of CD4⁺ Th1 cells was also observed *in vivo* as revealed from the higher frequencies of IFN- γ -producing OVA-specific CD4⁺ T cells in the spleens of OVA-Le^x immunized mice than in mice immunized with native OVA (Figure 3C, Figure 3-figure supplement 2). These data indicate that the increased numbers of Th1 cells induced by OVA-Le^x-loaded DCs are not due to increased proliferation of OT-II cells, but probably due to MGL1-mediated signaling.

MGL1 mediates cross-presentation of OVA-Le^x independently of TLR signaling

Since we observed a great enhancement of antigen-specific CD8⁺ T cell priming *in vivo* when immunizing with OVA-Le^x to target MGL1, we wanted to reveal the mechanism that regulates this augmented cross-priming. The internalization of OVA by BM-DCs was significantly increased when OVA was modified with Le^x (Figure 4A, Figure 4-figure supplement 1). To investigate whether the addition of Le^x glycans affected the efficiency of cross-presentation of OVA by DCs, we loaded murine BM-DCs or spDCs with OVA-Le^x and measured their potency to present OVA-derived peptides in MHC class I by measuring the proliferation of OVA-specific OT-I T cells. Strikingly, both BM-DCs as well as spDCs induced substantially more proliferation of OT-I T cells when they were pulsed with OVA-Le^x compared to native OVA (Figure 4B, Figure 4-figure supplement 2). Even at low concentrations of antigen (*i.e.* 7.5 $\mu\text{g/ml}$), the proliferating OT-I T cells were doubled (30% to 60%) using OVA-Le^x compared to using OVA (Figure 4B), indicating that the modification of OVA with Le^x greatly affected the cross-presentation of OVA. Moreover, detection of SIINFEKL/H-2K^b complexes on the cell membrane of OVA-Le^x-loaded DCs by staining with the 25.1D1 antibody confirmed enhanced antigen loading on MHC-I molecules and transportation to the cell-surface of internalized OVA-Le^x compared to native OVA (Figure 4C, Figure 4-figure supplement 3). Cross-presentation of OVA-Le^x was clearly mediated by MGL1 as demonstrated using MGL1 KO BM-DCs or steady-state spDCs (Figure 4D).

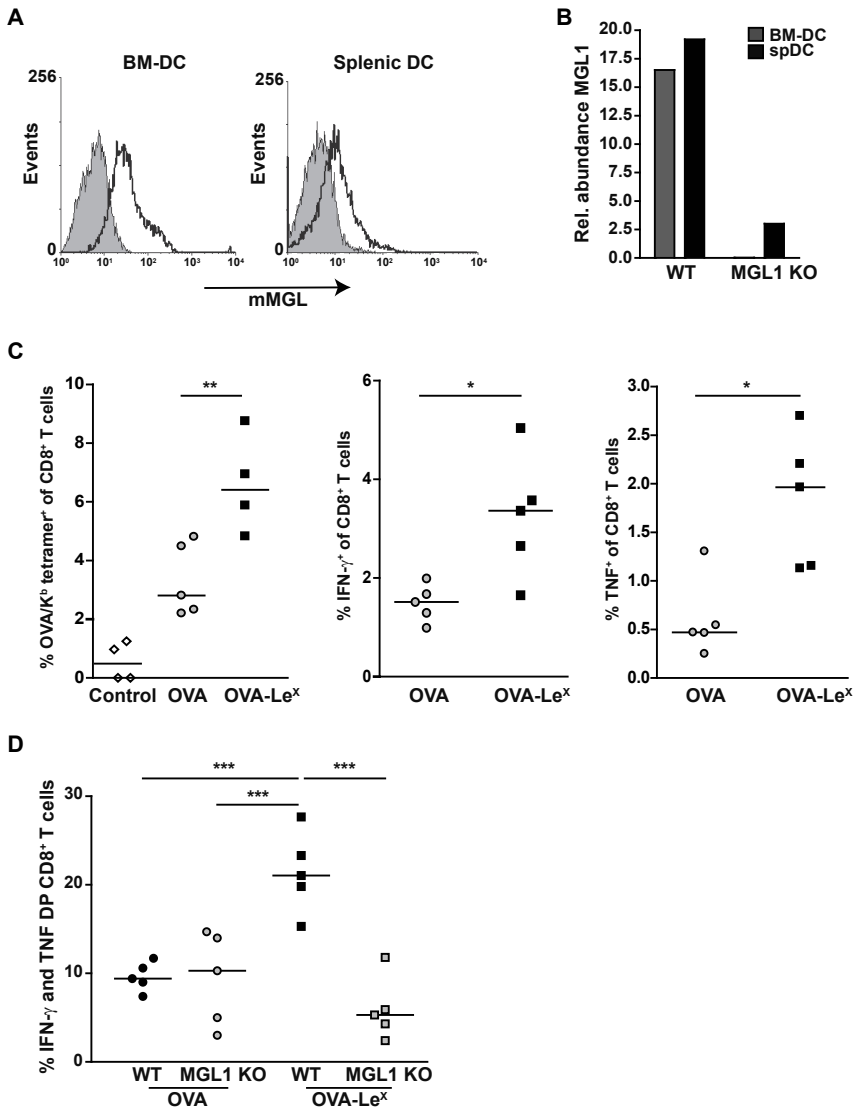


Figure 2. Immunization with OVA-Le^x induces increased CD8⁺ T cell responses *in vivo*. (A) Expression of murine MGL on BM-DCs and CD11c⁺ spDCs was analyzed by flow cytometry. (B) MGL1 mRNA expression by BM-DCs and splenic DCs from WT and MGL1 KO mice was determined using qRT-PCR. GAPDH was used as a reference gene and results are representative of three independent experiments. (C) C57BL/6 mice were immunized s.c. with either OVA-Le^x or native OVA mixed with anti-CD40 using a prime-boost protocol. Splensens were analyzed by flow cytometry to determine the frequency of H2-K^b/SIINFEKL-tetramer-binding CD8⁺ T cells and IFN- γ or TNF production by activated CD8⁺ T cells was determined by intracellular staining after OVA-specific re-stimulation *ex vivo*. Dots represent individual mice (n=4-5 mice/group; **, P<0.01). Bars indicate median of each group. Graphs shown are representative of two independent experiments. (D) C57BL/6 and MGL1 KO mice were prime-boosted with either OVA-Le^x or native OVA mixed with anti-CD40. Frequencies of IFN- γ and TNF-double-producing CD8⁺ T cells were determined by intracellular staining after OVA-specific re-stimulation of splenocytes *ex vivo*. Dots represent individual mice (n=4-5 mice/group; * P<0.05, *** P<0.001). Bars indicate median of each group. Data are representative of 2 independent experiments.

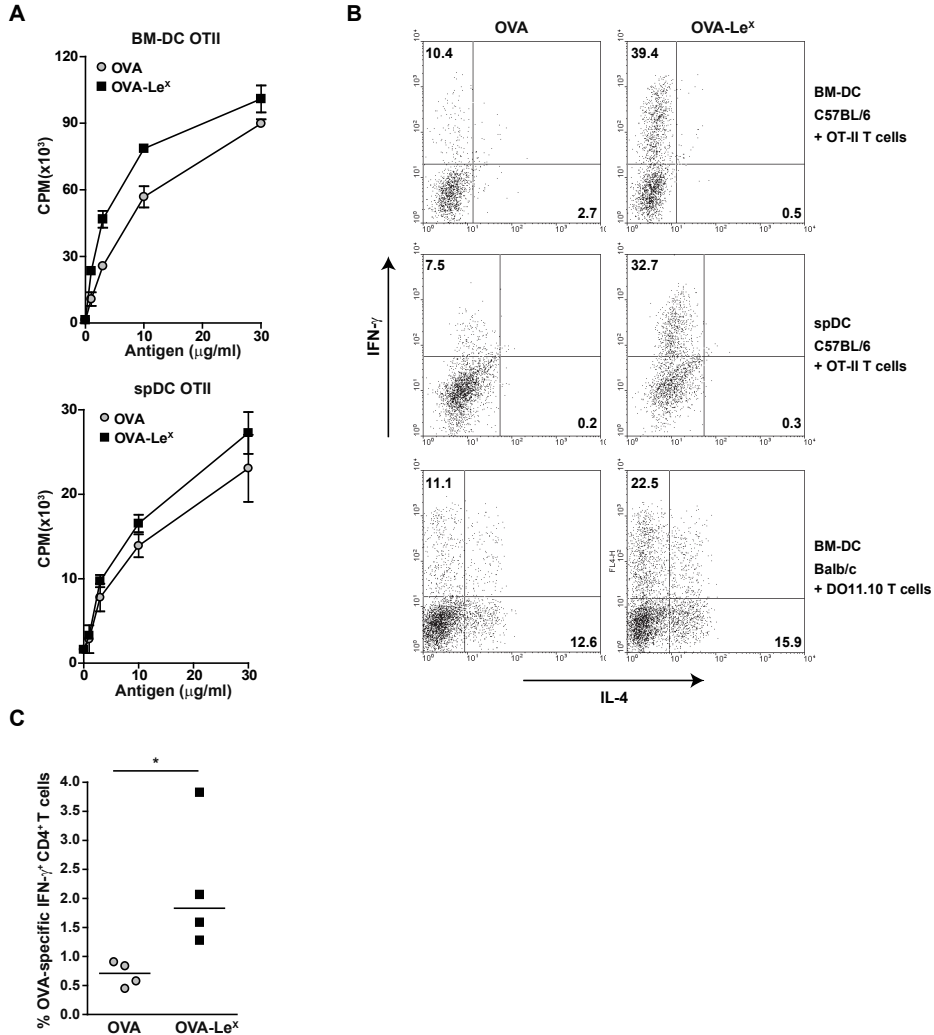


Figure 3. Modification of OVA with Le^x structures skews naive CD4⁺ T cells towards the Th1-effector lineage. (A) Pulsing of CD11c⁺ spDCs or BM-DCs with OVA-Le^x results in equal OT-II proliferation as native OVA. Expansion of OVA-specific T cells was determined using ³H-thymidine incorporation. Data are shown as mean \pm SD of triplicate cultures, representative of three independent experiments. **(B)** Flow cytometric analysis of OT-II or DO11.10 T cells differentiated by OVA-Le^x or OVA-loaded spDCs or BM-DCs. Cells were gated on CD4⁺ T cells. Numbers in dot plots indicate the percentage of IFN- γ ⁺ or IL-4⁺ of CD4⁺ T cells. Dot plots are representative of five independent experiments. **(C)** C57BL/6 mice were immunized s.c. with either OVA-Le^x or native OVA mixed with anti-CD40 using a prime-boost protocol and the frequency of IFN- γ -producing activated CD4⁺ T cells in spleen was determined by intracellular staining after OVA-specific re-stimulation *ex vivo*. Dots represent individual mice, bars indicate median of each group (n=5 mice/group, **P<0.01). Graphs shown are representative of two independent experiments

Cross-presentation of OVA via the MR was shown previously to be dependent on TLR signaling and the presence of high amounts of antigen ((34, 21, 37) and Figure 4-figure supplement 4, left panel). The observed differences in cross-presentation between OVA and OVA-Le^x were not due to any potential contamination with the TLR4 ligand LPS, as both protein preparations did not trigger IL-8 production by TLR4-transfected HEK293 cells (Figure 4-figure supplement 5). In addition, both OVA preparations neither induced maturation of BM-DCs nor altered their cytokine production (data not shown). To exclude any potential role of TLR signaling on the MGL1-mediated cross-presentation of OVA-Le^x we made use of BM-DCs from mice that lack both MyD88 and TRIF (*i.e.* MyD88/TRIF DKO). However, MyD88/TRIF DKO BM-DCs still induced more OT-I proliferation when targeted with OVA-Le^x than with OVA (Figure 4E) and only a slight reduction of cross-presentation was observed compared to that induced by WT BM-DCs, suggesting a minor role for MyD88- or TRIF-signaling in MGL1-induced cross-presentation. In line with previous findings, neither exogenous loading of MHC-I molecules with OVA257-264 peptides (Figure 4E) nor MHC class II presentation of OVA-Le^x and OVA was dependent on MyD88- or TRIF- signaling and resulted in comparable expansion of OVA-specific T cells (data not shown).

Cross-presentation induced by MGL1-targeting is independent of TAP-transport and cathepsin S-induced endosomal degradation

Several cross-presentation pathways have been described, one of which is dependent on the transport of peptides from the cytosol into MHC-class I loading compartments via TAP-molecules (38, 39), whereas another cross-presentation pathway depends on endosomal degradation by the cysteine protease cathepsin S (40). To study a role for TAP transporters in our model, BM-DCs of TAP-1 KO and WT control mice were pulsed with OVA-Le^x followed by incubation with OT-I T cells. Surprisingly, cross-presentation induced by OVA-Le^x was not reduced by the absence of TAP as OT-I proliferation induced by OVA-Le^x-loaded TAP-1 KO BM-DCs was not decreased compared to OVA-Le^x-loaded WT BM-DCs (Figure 5A). In accordance with previous publications (21) we showed that administration of OVA with LPS is cross-presented in a TAP-dependent manner (Figure 4-figure supplement 4, right panel).

Furthermore, the possibility that the results are confounded by reduced levels of MHC-class I on TAP-1 KO BM-DCs was excluded as the presentation of exogenously loaded OVA257-264 peptide is equal by both WT and TAP-1 KO BM-DCs (Figure 5A). In addition, we excluded the involvement of the cathepsin S pathway for cross-presentation of OVA-Le^x as cross-presentation of OVA-Le^x by BM-DCs from cathepsin S KO mice (Cat-S KO) was not reduced compared to WT BM-DCs (Figure 5B). As expected, the MHC-class II-restricted CD4⁺ T cell proliferation was compromised in the Cat-S KO BM-DCs (data not shown), illustrating the involvement of cathepsin S in cleaving the invariant chain of the MHC-class II molecule (41).

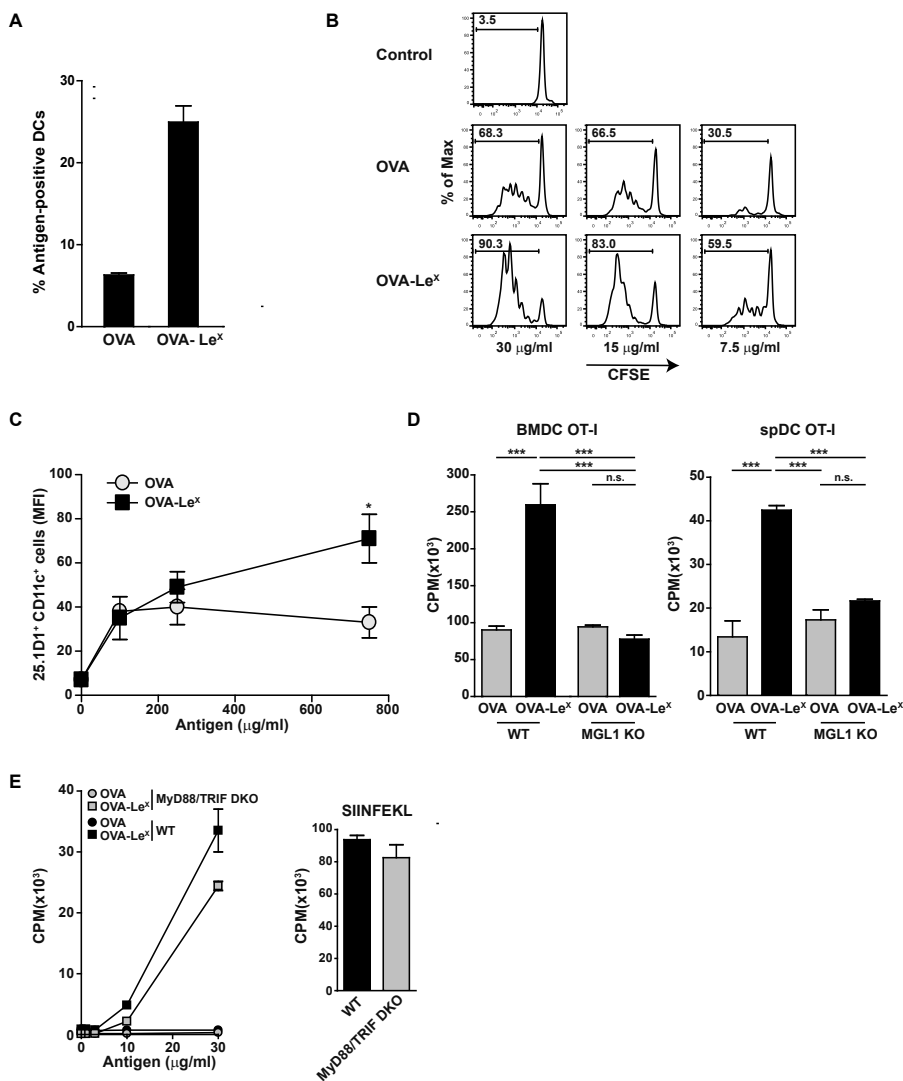


Figure 4. MGL1 mediates cross-presentation of OVA- Le^x independently of TLR signaling. (A) Uptake of fluorescent-labeled OVA- Le^x or native OVA (30 μ g/ml) by WT BM-DCs was analyzed by flow cytometry after 90 min. Graphs indicate the mean \pm SD of triplicates and are representative of three independent experiments. (B) CFSE-labeled OT-I T cells were incubated with BM-DCs pulse-loaded with indicated concentrations of OVA- Le^x or OVA for 4h. Un-loaded DCs served as controls. Proliferation of OT-I T cells was analyzed after 3 days by flow cytometry. Percentages of divided OT-I cells are indicated. (C) OVA- Le^x induces more OVA257-264/H2-K^b I complexes at the cell-surface of DCs than native OVA, as shown by 25.1D1 staining 18h after pulse loading of BM-DCs with OVA- Le^x or native OVA. * P <0.05. (D) WT or MGL1 KO BM-DCs or CD11c⁺ spDCs are pulsed with OVA- Le^x (black bars) or native OVA and OT-I proliferation was determined on day 3 by [³H]-thymidine uptake. Data are presented as mean \pm SD of triplicates, representative of three independent experiments. *** P <0.001, ns not significant. (E) Cross-presentation of OVA- Le^x is independent of MyD88 and/or TRIF signaling. BM-DCs from WT or MyD88/TRIF DKO mice were pulsed with indicated concentrations of antigen and co-cultured with OT-I T cells. DCs pulsed with the nominal epitope SIINFEKL served as controls (right panel). Proliferation was determined by [³H]-thymidine uptake. Data are representative of two experiments and indicated as mean \pm SD of triplicates.

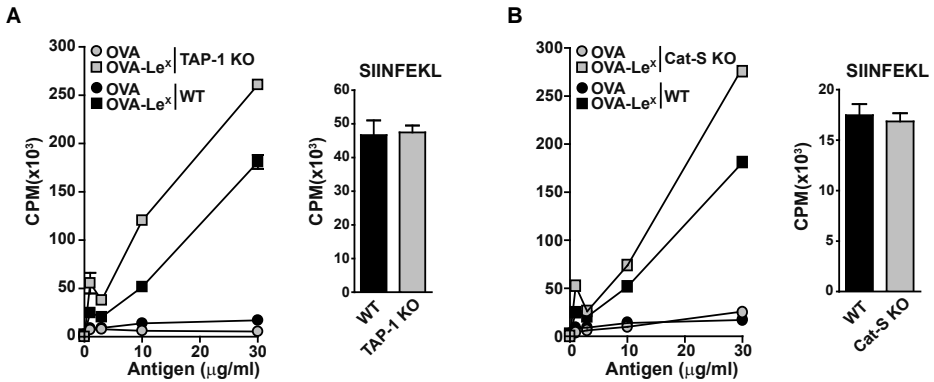


Figure 5. Le^x-modified antigen is cross-presented in a TAP- and cathepsin S-independent fashion. To examine whether cross-presentation of OVA-Le^x involves TAP or cathepsin S (A) TAP-1 KO and (B) Cat-S KO BM-DCs and WT BM-DCs were pulsed with OVA-Le^x or native OVA and co-cultured with OT-I T cells for 3 days. DCs exogenously loaded with SIINFEKL for 3h served as control. Proliferation was determined by [³H]-Thymidine uptake and data are presented as mean±SD of triplicates (representative of three experiments).

Modification of OVA with Le^x alters the intracellular routing of OVA

As the dominant cross-presentation of Le^x-modified OVA was neither dependent on TAP nor required TLR signaling, we hypothesized that this may be due to the altered uptake and intracellular routing of OVA in DCs. We therefore used imaging flow cytometry, a method that allows high-throughput image analysis of cells in flow with near-confocal resolution to analyze the intracellular routing of fluorescent labeled OVA-Le^x. Co-staining with markers for early endosomal (EEA-1), late endosomal/lysosomal (LAMP1) and recycling endosomal (Rab11) compartments illustrated a swift co-localization of OVA-Le^x with EEA1 and Rab11 as shown by high co-localization scores at 15 min (Figure 6A, Figure 6-figure supplement 1). However, this co-localization score was strongly decreased after 60 min. At this time-point, higher co-localization scores were detected for OVA-Le^x with LAMP1 and Rab11 (Figure 6B, Figure 6-figure supplement 2). We then further dissected the intracellular pathway of OVA-Le^x using confocal laser scan microscopy (CLSM) and compared it to the intracellular routing of native OVA. We confirmed that native OVA, which internalized via MR, was routed to EEA1⁺Rab11⁺ compartments within two hours (Figure 6C, upper-left panel and (21)). However, the neoglycosylation with Le^x altered the intracellular routing of OVA, showing its presence predominantly within LAMP1⁺Rab11⁺ compartments (Figure 6C, upper-right panel). Moreover, OVA-Le^x internalized by BM-DCs from MGL1 KO mice was routed to EEA1⁺Rab11⁺ compartments and did not end up in LAMP1⁺Rab11⁺ compartments, similar to OVA in WT BM-DCs (Figure 6C, lower panels, Figure 6-figure supplement 3). Together, these data suggest that upon internalization, OVA-Le^x is rapidly shuttled to Rab11⁺EEA1⁺ compartments from where it moves to Rab11⁺LAMP1⁺ compartments, where it persists for

longer periods (*i.e.* >24h). Thus, these results indicate that internalization via MGL1 allows the antigen to enter the endosomal/lysosomal pathway. The development of early endosome into late endosome/lysosome coincides with a decreasing pH gradient. The pH at which MGL1 dissociates from its ligand is indicative of the compartment in which the antigen becomes available for degradation and loading on MHC-molecules. We therefore analyzed MGL1-binding to its ligand Le^x at different pH that resembled the pH of the intracellular compartments. MGL1 starts dissociating from Le^x already at pH 6.5 (Figure 6D). This indicates that OVA-Le^x becomes available for degradation in the early and late endosomal compartments, compartments both associated with cross-presentation.

The sustained presence of OVA-Le^x in Rab11⁺LAMP1⁺ compartments (Figure 6B and C) prompted us to investigate whether these compartments facilitate prolonged cross-presentation, as shown by van Montfoort *et al.* for OVA-immune complexes (42). Indeed, even two days after antigen pulse, OVA-Le^x-loaded DCs induced strong expansion of OT-I T cells, suggesting that OVA-Le^x-loaded DCs have prolonged cross-presentation capacity (Figure 7A). At the highest antigen concentration used (*i.e.* 30 µg/ml), the percentage of proliferated OT-I T cells was only slightly reduced 48h after pulse compared to that induced by DCs that were pulsed with OVA-Le^x for 4h (Figure 7A). Expansion of OT-I T cells driven by 48h pulse loaded DCs was even detectable at low antigen concentrations (3.75 µg/ml). OT-II proliferation induced by DCs pulsed with OVA-Le^x for 48h was also still detectable although less pronounced than the OT-I induced proliferation (Figure 7B), suggesting that the prolonged storage of antigen in these intracellular compartments predominantly favored cross-presentation. Taken together, these data suggest that antigen internalized by MGL1 is routed from Rab11⁺EEA1⁺ compartments towards Rab11⁺LAMP1⁺ compartments, which seem to associate with the extended antigen-processing and cross-presentation.

DISCUSSION

We here demonstrate that the glycosylation-profile of antigens has a major influence on antigen uptake and intracellular compartmentalization, thereby affecting both antigen presentation and the type and strength of the induced immune response. Modification of the model-antigen OVA with Le^x glycans directs OVA towards MGL1, skewing naive CD4⁺ T cell differentiation towards IFN γ -producing Th1 cells. Moreover, targeting OVA to MGL1 through the conjugation of Le^x, substantially enhanced cross-presentation as revealed by the increased frequency of OVA-specific CD8⁺ effector T cells *in vitro* and *in vivo*. Importantly, MGL1-dependent cross-presentation occurred at low antigen dose and independently of TLR-signaling. Moreover, this cross-presentation pathway did not involve TAP-transporters and cathepsin S. MGL1 targeting involved antigen routing to a Rab11⁺LAMP1⁺ compartment in which antigen was present for prolonged periods.

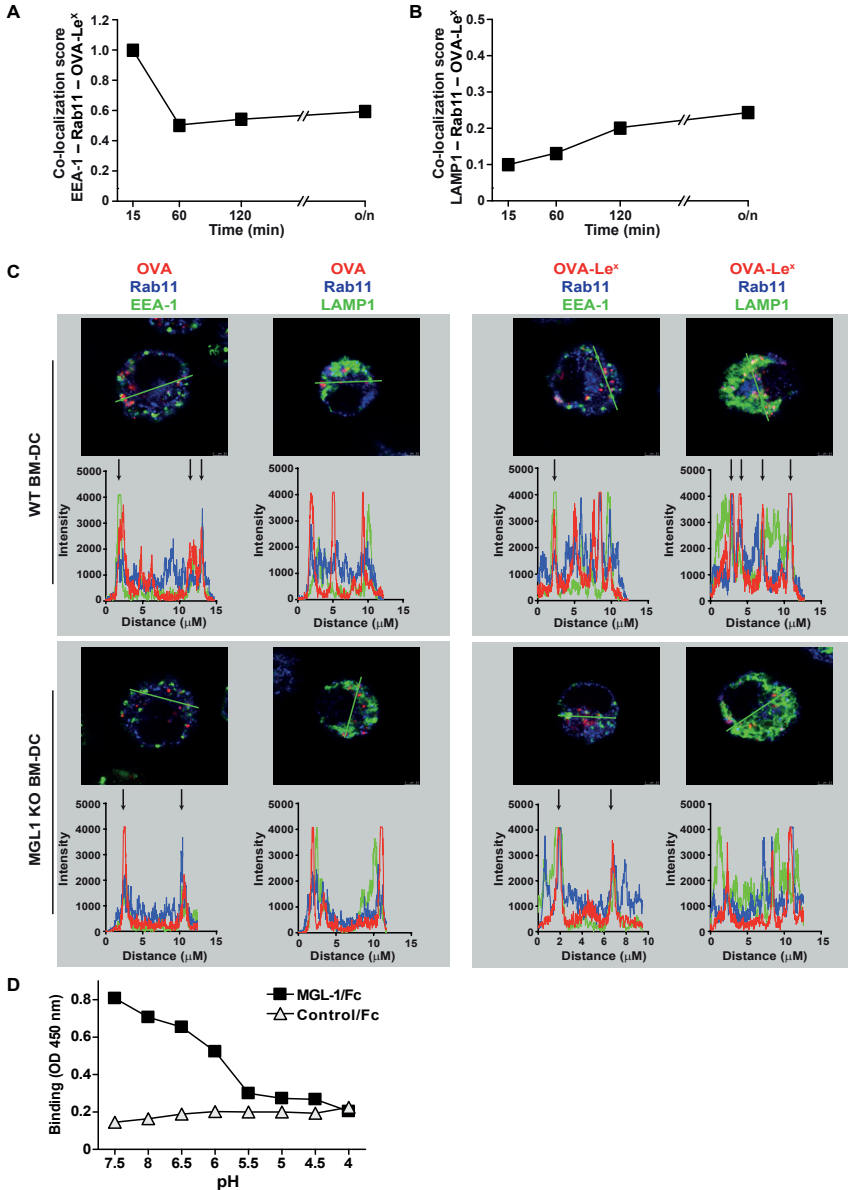


Figure 6. OVA-Le^x is routed to Rab11⁺LAMP1⁺ compartments where it is stored for presentation in MHC class I. (A, B) WT BM-DCs were pulsed with Alexa Fluor 674-OVA-Le^x (30 µg/ml) and chased at the indicated time-points to assess triple co-localization scores of OVA-Le^x with (A) EEA-1 and Rab11 or (B) LAMP1 and Rab11 using imaging flow cytometry. (C) WT (upper panels) and MGL1 KO (lower panels) BM-DCs were incubated with Dylight-633-OVA-Le^x or native OVA (30 µg/ml) and 2h later co-localization of OVA antigen (Red) with early endosomal (EEA-1, Green) or endosomal/lysosomal (LAMP1, Green) and recycling endosomal (Rab11, Blue) compartments was analyzed using CSLM. From a z-stack, histograms were created for a selected area (indicated by a line, upper part of each panel) using the Leica confocal software. Histograms were created from each fluorochrome and overlays were made by the program. Arrows indicate co-localization of antigen (Red) with EEA1&Rab11 or LAMP1&Rab11. (D) MGL1-Fc binding to Le^x-PAA was determined at indicated pH by ELISA.

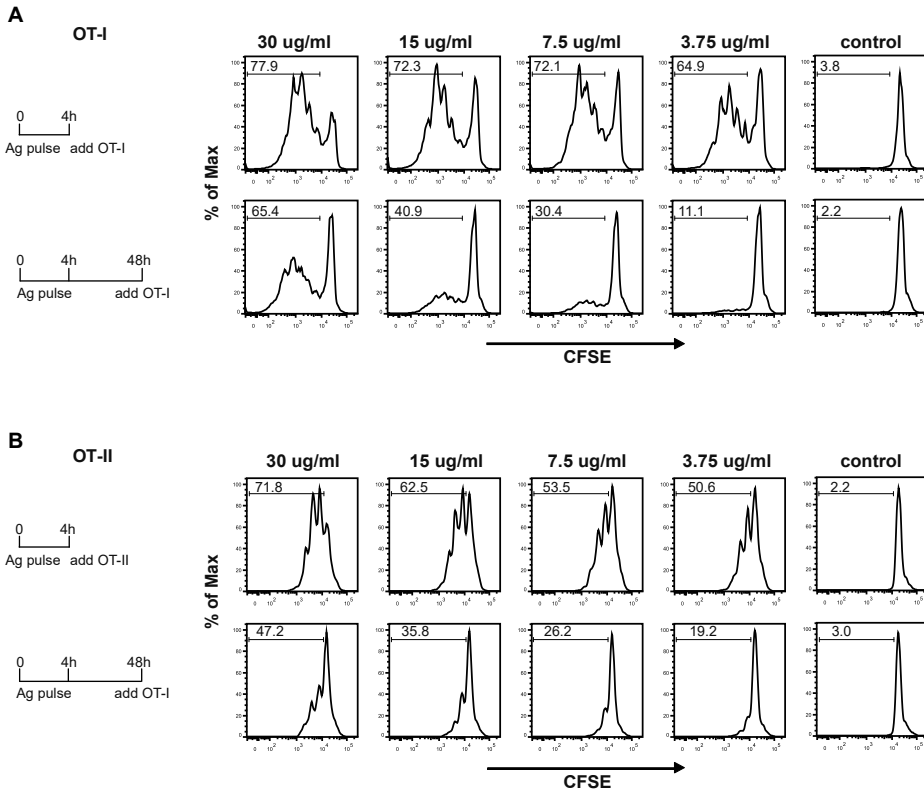


Figure 7. MGL1 targeting with OVA-Le^x shows sustained antigen presentation in MHC-I. WT BM-DCs were pulsed for 4h with titrated amounts of OVA-Le^x and washed with culture medium. DCs were then chased for 48h in antigen-free medium. **(A)** BM-DCs pulsed for 4h with OVA-Le^x induced MHC-I antigen presentation as measured by CFSE-labeled OVA-specific OT-I cells (upper panel). Sustained presentation is shown after 48h (lower panel). **(B)** MHC-II antigen presentation 4h and 48h after pulse-loading with OVA-Le^x, analyzed by OT-II proliferation. Data are presented as percentage of proliferated T cells and representative of three independent experiments.

Previous studies on CLR-mediated antigen uptake and cross-presentation, in particular by the MR, demonstrated a clear requirement for a TLR ligand (43, 21, 44, 45). A common denominator in some of these studies is that the use of antibody-antigen conjugates could potentially induce a different signal than the natural ligand, due to binding to different part of the receptor or through co-engagement of Fc-receptors. The fact that the addition of Le^x glycans to OVA obviates the need for TLR signals for the induction of cross-presentation and Th1 priming *in vitro*, may indicate that MGL1 signaling is involved in these processes. Some CLR, like DC-SIGN, Clec9A and Dectin-1 are known to induce signaling after triggering by their natural ligands (9, 46). Till now, no signaling pathway has been described for MGL1. Triggering of huMGL resulted in ERK1/2 and NF- κ B activation, and results in elevated levels of IL-10 and TNF (47, 48). In our studies the uptake of Le^x-modified OVA through MGL1 was

not associated with any DC maturation or altered cytokine production by DCs. The fact that OVA-Le^x induced an enhanced frequency of Th1 cells *in vitro* and of antigen-specific effector T cells *in vivo* when combined with agonistic anti-CD40 Abs illustrates that a yet to be determined costimulatory signal is essential for the induction of effector CD8⁺ and CD4⁺ T cells. This powerful function of MGL1 to establish antigen-specific immunity, stands opposite to its recently demonstrated anti-inflammatory function, which include induction of IL-10 production and altered adhesive function by APC (49, 50).

Various models for cross-presentation of antigens have been contemplated. The “cytosolic pathway” of cross-presentation allows receptor-mediated endocytosis or phagocytosis and antigen translocation into the cytosol, where they are degraded into antigenic peptides by the proteasome and transported into the lumen of the endoplasmic reticulum (ER) (43, 40) or ER/phagosomal fusion compartments (51, 52) by TAP-transporters. A variation to the cytosolic pathway was described in which soluble OVA is taken up via the MR and is supplied to stable early endosomal compartments (22). In these compartments, the MHC class I machinery as well as TAP-transporters are selectively recruited, facilitating direct loading of antigen-derived peptides onto MHC class I molecules without trafficking to the ER. The “vacuolar pathway” allows antigens to be degraded into peptides in early endosomal compartments by endosomal proteases like cathepsin S, to be loaded on MHC class I molecules in the same compartment, thus is TAP-independent (40). The current described models for cross-presentation depend on peptide-transport by TAP from the cytosol to either ER or ER/phagosomal fusion compartments or on endosomal degradation of antigens via cathepsin S (reviewed in (38, 53, 54, 39)). Although we observed localization of OVA-Le^x in early endosomes, absence of either TAP molecules or cathepsin S did not influence the enhanced cross-presentation of OVA-Le^x. Our data indicate that the MGL1 cross-presentation pathway is different than that of the MR and may occur via antigen storage compartments similar to those described for FcγR-targeted antigens (42). We observed prolonged presence in Rab11⁺LAMP1⁺ compartments in the absence of a maturation stimulus or apparent DC maturation. It is tempting to speculate that in these compartments cross-presentation of OVA is facilitated by Rab11 as it was recently shown that Rab11 activity mediates delivery of MHC-I molecules to phagosomes used for cross-presentation during infection (55). However, recruitment of additional components involved in antigen cross-presentation by the SNARE Sec22b40 complex cannot be excluded (56). The prolonged antigen cross-presentation via MGL1 allows sustained cross-priming of CD8⁺ T cells *in vivo* and thus the efficacy of tumor vaccines that target MGL1 may be higher than of conventional vaccines containing non-targeted antigens.

In the current study, we show that already at very low concentrations, soluble protein antigens are efficiently cross-presented upon uptake by MGL1. DCs pulsed with a low dose of OVA-Le^x (7.5 μg/ml) induced significant CD8⁺ T cell proliferation, whereas

the same concentration of native OVA was hardly cross-presented (Figure 4). Others have demonstrated that native OVA can only be cross-presented when a high dose was used (0.5-1.0 mg/ml) and when accompanied with TLR-triggering (21, 45). Although the glycan-modification was associated with increased antigen uptake and enhanced cross-presentation, it did not result in enhanced presentation of antigen on MHC-class II indicating that increased uptake of antigen is not per se a requirement to facilitate MHC class I and II presentation. Therefore, it is most likely that the CLR (and thus the glycosylation of the antigen) dictates how efficiently an antigen is cross-presented. Based on our study MGL1 cross-presents antigen much more efficiently than the MR. The activity of the glycosylation machinery is subjected to subtle regulation and depends on the cell-type or activation status of the cell. Upon malignant transformation glycan profiles may change dramatically. Le^x carbohydrate structures are described to be expressed in the brain (57), and can be *de novo* expressed on cancer stem cells (58) or pathogens, and the glycosylation pattern of *in vivo* accumulating antigens, being brain tissue, tumor tissue or pathogen structure, is crucial for directing specific CLR antigen uptake and cross-presentation (59, 60). Although in our studies only two Le^x glycans were conjugated to each OVA molecule, it cannot be ruled out that multivalent presentation of Le^x, such as often observed on tumors or pathogens (61, 62), may alter avidity-induced MGL-1 signaling and antigen presentation, and induce an anti-inflammatory immune repertoire. At this stage we do not know whether high glycan valency further enhances or inhibits the MGL1-mediated (cross-) priming.

The fact that pulsing of DCs with OVA-Le^x resulted in improved cross-priming and Th1-skewing indicates that conjugation of these carbohydrates to tumor-antigens could be beneficial for induction of potent anti-tumor responses. Therefore, the use of glycans for targeting CLR for anti-cancer immunotherapy could have several advantages. First, they mimic natural function of the receptors, inducing 'natural' signaling cascades in DCs. Furthermore, they are very small molecules, easy to use and relatively cheap to produce. Importantly, many glycans may be considered self-antigens, in contrast to recombinant antibodies that are often not completely of human origin. These properties make it possible to decorate any antigen of choice with glycans to target specific receptors.

In conclusion, our studies indicate that the glycan composition of protein antigens is of fundamental importance in dictating the intracellular routing and Th-skewing, and should be considered as a major determinant in the design of therapeutic vaccines against cancer and infectious diseases.

MATERIALS AND METHODS

Mice

C57BL/6 mice (Charles River Laboratories) were used at 8-12 weeks of age. MGL1 KO mice, which have a null mutation within the *Clec10a* gene, are on the C56BL/6 background and were kindly provided through the Consortium for Functional Glycomics. TAP-1 KO mice have a null mutation within the *Tap1* gene. MGL1 KO, TAP-1 KO, OT-I and OT-II TCR transgenic mice were bred in our animal facilities under specific pathogen-free conditions. All experiments were performed according to institutional, state and federal guidelines.

Antibodies and Fc-chimeric constructs

Fluorochrome-conjugated antibodies used: anti-CD11c-APC, anti-IFN γ -APC, anti-TNF α -PE-cy7, anti-IL-4-PE, anti-IL17-PE, anti-Foxp3-PE (e-Bioscience), and anti-LAMP-1-v450 (BD-Pharmingen). Unconjugated mouse anti-OVA (Sigma Aldrich), mouse anti-Le^x (Calbiochem), rat anti-mMGL (ER-MP23; kind gift from Dr. P. Leenen, Erasmus MC, Rotterdam, The Netherlands), rat anti-LAMP1 (BD-Pharmingen), rabbit anti-Rab11 (Life Technologies), goat anti-EEA1 (Santa Cruz Biotechnology) and rabbit anti-EEA-1 (Dianova). Secondary antibodies used: peroxidase-labeled F(ab')₂ fragment goat anti-human IgG, F(ab')₂ fragment goat anti-mouse IgG, (Jackson), peroxidase-labeled goat anti-mouse IgM (Nordic Immunology), goat anti-rat Alexa 448, goat anti-rat Alexa 647, donkey anti-goat Alexa488, donkey anti-goat Alexa 647, donkey anti-rabbit Alexa 555 and donkey anti-rabbit Alexa 488 (Molecular Probes). MGL-1-Fc was generated as described earlier (24). MR-Fc was kindly provided by L. Martinez-Pomares (University of Nottingham, Nottingham, UK).

Generation of neo-glycoconjugates

Le^x (lacto-N-fucopentose III; Dextra Labs, UK) carbohydrate structures were conjugated to OVA (Calbiochem) as previously described (14). In short, the bifunctional cross-linker (4-*N*-maleimidophenyl) butyric acid hydrazide (MPBH; Pierce) was covalently linked to the reducing end of the Le^x and the maleimide moiety of the linker was later used for coupling the Le^x to OVA. Neo-glycoconjugates were separated from reaction by-products using PD-10 desalting columns (Pierce). Additionally, a Dylight 549-*N*-hydroxysuccinimide (NHS) label (Thermo Scientific) was covalently coupled to OVA or OVA-Le^x (Dylight-549-OVA). Free label was removed using a PD-10 column (Pierce). The presence of Le^x and CLR binding to OVA was measured by ELISA. In brief, OVA-conjugates were coated directly on ELISA plates (NUNC) and binding of MR-Fc, MGL1-Fc, anti-Le^x and anti-OVA antibodies to OVA was determined as described (14, 11). The presence of endotoxin was measured using a LAL assay (Lonza) following manufacturer's protocol.

Glycan analysis

OVA was deglycosylated by incubation in 5 IU of PNGase F (Roche Applied Sciences) o/n at 37°C. Proteins were extracted by reverse phase chromatography using Sep-Pak Vac C18 disposable cartridges (Waters). Glycans were further purified by reverse phase chromatography using Superclean ENVI-Carb cartridges disposable columns (Supelco). Glycans were lyophilized and re-dissolved in 30 ml of 7-Amino-4-methylcoumarin (160 mM, Sigma Aldrich) and 2-Picoline borane (270 mM, Sigma Aldrich) in DMSO:acetic acid (4:1, Riedel deHaën). 4-AMC-labelled glycans were purified by size exclusion chromatography using a Bio-Gel P2 (Bio-Rad) column with 50 mM ammonium formate (Sigma Aldrich) as running buffer. 4-AMC-labelled glycans were lyophilized and analyzed by multidimensional normal phase HPLC (UltiMate 3000 nanoLC, Dionex) using a Prevail Carbohydrate ES 0.075 x 200 mm column (Grace) coupled to an LCQ Deca XP with electrospray interface mass spectrometer (Thermo Finnigan) tuned with maltoheptaose (Sigma Aldrich) labeled with 4-AMC and with an intercalated fluorescence detector (Jasco FP-2020 Plus, Jasco) (maximum excitation 350 nm, band width 40 nm; maximum emission 448 nm, band width 40 nm) as previously described (63).

Molecular weight determination

Matrix-assisted laser desorption/ionization-time of flight (MALDI-TOF) mass spectrometry measurements were done using a 4800 MALDI-TOF/TOF Analyzer (Applied Biosystems). Mass spectra were recorded in the range from 19000 to 155000 m/z in the linear positive ion mode. The data were recorded using 4000 Series Explorer Software and processed with Data Explorer Software version 4.9 (all from Applied Biosystems).

Immunization of mice

C57BL/6 or *Mgl1^{-/-}* mice were injected s.c. either with 100 µg OVA-Le^x or OVA mixed with 25 µg anti-CD40 Ab (1C10) on day 0 and day 14. Mice were sacrificed one week after boost and the amount of antigen-specific CD8⁺ T cells was analyzed in the spleen by staining with H2-Kb-SIINFEKL tetramers (Sanquin). Additionally, frequencies of OVA-specific cytokine-secreting T cells were analyzed by flow cytometry. Hereto, spleen cells were re-stimulated overnight with either 2 µg/ml SIINFEKL or 200 µg/ml EKLTEWTSSNMEER OVA peptides in the presence of 5µg/ml Brefeldin A, then IFN-γ and TNFα expression were assessed by intracellular staining using specific antibodies.

Cells

BM-DCs were cultured as previously described (14). BM of *Myd88/Ticam1* DKO (referred to as MyD88/TRIF DKO) and *Ctss^{-/-}* (referred to as Cat-S KO) mice was kindly provided by Dr. T. Sparwasser (Twincore, Hannover, Germany) and Dr. K. Rock (Massachusetts Medical School,

Worcester, MA, USA), respectively. CD11c⁺ spDCs were isolated as previously described (Singh et al., 2009a). OVA-specific CD4⁺ and CD8⁺ T cells were isolated from spleen and lymph nodes cell suspensions from OT-II and OT-I mice, respectively using the mouse CD4 and CD8 negative isolation kit (Invitrogen, CA, USA) according to manufacturer's protocol. T cell proliferation assays were performed as described (14). In short, DCs were pulsed with OVA-Le^x or OVA for 4h before incubation with OVA-specific OT-I or OT-II T cells (2:1 DC:T). [³H]-Thymidine (1 μCi/well; Amersham Biosciences) was present during the last 16h of a 72h culture. [³H]-Thymidine incorporation was measured using a Wallac microbeta counter (Perkin-Elmer). Alternatively, OT-I or OT-II T cells were labeled with CFSE and after 3 days dilution of CFSE was analyzed by flow cytometry. Differentiation of naive OT-II T cells, induced by OVA-Le^x or OVA-pulsed BM-DCs or spDCs, was measured by an in vitro Th differentiation assay described earlier (20).

cDNA synthesis and Real-Time PCR

mRNA was isolated by capturing poly(A⁺)RNA in streptavidin-coated tubes using a mRNA Capture kit (Roche, Basel, Switzerland). cDNA was synthesized using the Reverse Transcription System kit (Promega, WI, USA) following manufacturer's guidelines. Real-Time PCR reactions were performed using the SYBR Green method in an ABI 7900HT sequence detection system (Applied Biosystems).

Confocal microscopy and imaging flow cytometry

BM-DCs were incubated with 30 μg/ml Dylight-633-OVA or OVA-Le^x for 30min or 2h at 37°C, fixed and permeabilized for 20 min on ice, and stained with primary and secondary antibodies. Co-localization was analyzed using a confocal laser scanning microscope (Leica SP5 STED) system containing a 63x objective lens; images were acquired in 10x magnification and processed with Leica LAS AF software. For imaging flow cytometry, approximately 1x10⁶ BM-DCs were incubated with OVA-Le^x for 30 min at 4°C, washed twice in ice-cold PBS and then transferred to 37°C. At the indicated time-points cells were washed twice and fixated in ice-cold 4% paraformaldehyde (PFA, Electron Microscopy Sciences) in PBS for 20 min. Cells were then permeabilized in 0.1% saponin (Sigma) in PBS for 30 min at RT and subsequently blocked using PBS containing 0.1% saponin and 2% BSA for 30 min at RT. Stainings were performed at room temperature (RT) in PBS supplemented with 0.1% saponin and 2% BSA. After staining, cells were washed twice in PBS, resuspended in PBS containing 1% BSA and 0.02% NaN₃ and kept at 4°C until analysis. Cells were acquired on an ImageStream X100 (Amnis) imaging flow cytometer. A minimum of 15000 cells was acquired per sample at a flow rate ranging between 50 and 100 cells/second at 60x magnification. At least 2000 cells were acquired from single stained samples to allow for compensation. Analysis was performed using the IDEAS v6.1 software (Amnis). Cells were first gated based on the Gradient RMS

(brightfield) feature and then based on area vs aspect ratio intensity (both on brightfield). The first gating identified the cells that appeared in focus, while the second excluded doublets and cells other than BM-DCs. 3-colour co-localization was calculated using the bright detail co-localization 3 feature.

pH dependency of MGL1 binding

The pH dependency of MGL1 binding to Le^x on antigens was determined by ELISA. Hereto, Le^x-PAA (Lectinity Holdings) was coated onto NUNC Maxisorp plates o/n at RT. Plates were blocked with 1% BSA in TSM buffer (20 mM Tris-HCl; 150 mM NaCl; 2 mM CaCl₂; 2 mM MgCl₂). After washing, MGL1-Fc was added in TSA with different pH and were kept in this buffer throughout the assay. Binding was detected using peroxidase-labeled F(ab')₂ fragment goat anti-human IgG.

Statistical analysis

Graphpad prism 5.0 was used for statistical analysis. The Student's t-test and one-way ANOVA with Bonferroni correction were used to determine statistical significance. Statistical significance was defined as $P < 0.05$.

ACKNOWLEDGEMENTS

We thank Sandra van Vliet for critical reading of the manuscript. This research was supported by VENI-NWO-ALW (grant 863.08.020 to J.J.G.V.), Senternovem SII071030 to W.W.J.U, Mozaiek 017.001.136 to S.K.S, AICR 07-0163 to E.S.

AUTHOR CONTRIBUTIONS

I.S-O designed and performed experiments, analyzed and interpreted data, and wrote paper; N.I.H., M.B. and L.A.M.C. performed experiments, analyzed and interpreted data; M.L., R.R., and S.K.S. performed experiments; H.K. produced glycan-antigen conjugates; J.J.G.V. performed glycan-analysis and imaging flow cytometric analysis and analyzed and interpreted data; E.S. and F.O. designed experiments and interpreted data; W.W.J.U. and Y.v.K. designed experiments, interpreted data, wrote paper and supervised the study.

REFERENCES

1. Carbone, F. R., and M. J. Bevan. Class I-restricted processing and presentation of exogenous cell-associated antigen in vivo. *J. Exp. Med.* 1990. 171: 377–387.
2. Bennett, S. R. M., F. R. Carbone, F. Karamalis, J. F. A. P. Miller, and W. R. Heath. Induction of a CD8+ cytotoxic T lymphocyte response by cross-priming requires cognate CD4+ T cell help. *J. Exp. Med.* 1997. 186: 65–70.
3. Schoenberger, S. P., R. E. M. Toes, E. I. H. Van Dervoort, R. Offringa, and C. J. M. Melief. T-cell help for cytotoxic T lymphocytes is mediated by CD40-CD40L interactions. *Nature* 1998. 393: 480–483.
4. Apweiler, R., H. Hermjakob, and N. Sharon. On the frequency of protein glycosylation, as deduced from analysis of the SWISS-PROT database. *Biochim. Biophys. Acta - Gen. Subj.* 1999. 1473: 4–8.
5. Ohtsubo, K., and J. D. Marth. Glycosylation in Cellular Mechanisms of Health and Disease. *Cell* 2006. 126: 855–867.
6. van Kooyk, Y., and G. A. Rabinovich. Protein-glycan interactions in the control of innate and adaptive immune responses. *Nat. Immunol.* 2008. 9: 593–601.
7. Engering, A., T. B. H. Geijtenbeek, S. J. van Vliet, M. Wijers, E. van Liempt, N. Demaurex, A. Lanzavecchia, J. Fransen, C. G. Figdor, V. Piguët, and Y. van Kooyk. The Dendritic Cell-Specific Adhesion Receptor DC-SIGN Internalizes Antigen for Presentation to T Cells. *J. Immunol.* 2002. 168: 2118–2126.
8. Herre, J., A. S. J. Marshall, E. Caron, A. D. Edwards, D. L. Williams, E. Schweighoffer, V. Tybulewicz, C. Reis E Sousa, S. Gordon, and G. D. Brown. Dectin-1 uses novel mechanisms for yeast phagocytosis in macrophages. *Blood* 2004. 104: 4038–4045.
9. Geijtenbeek, T. B. H., and S. I. Gringhuis. Signalling through C-type lectin receptors: Shaping immune responses. *Nat. Rev. Immunol.* 2009. 9: 465–479.
10. Bonifaz, L. C., D. P. Bonnyay, A. Charalambous, D. I. Darguste, S.-I. Fujii, H. Soares, M. K. Brimnes, B. Molledo, T. M. Moran, and R. M. Steinman. In vivo targeting of antigens to maturing dendritic cells via the DEC-205 receptor improves T cell vaccination. *J. Exp. Med.* 2004. 199: 815–824.
11. Hawiger, D., K. Inaba, Y. Dorsett, M. Guo, K. Mahnke, M. Rivera, J. V Ravetch, R. M. Steinman, and M. C. Nussenzweig. Dendritic cells induce peripheral T cell unresponsiveness under steady state conditions in vivo. *J. Exp. Med.* 2001. 194: 769–779.
12. Caminschi, I., A. I. Proietto, F. Ahmet, S. Kitsoulis, J. Shin Teh, J. C. Y. Lo, A. Rizzitelli, L. Wu, D. Vremec, S. L. H. van Dommelen, I. K. Campbell, E. Maraskovsky, H. Braley, G. M. Davey, P. Mottram, N. van de Velde, K. Jensen, A. M. Lew, M. D. Wright, W. R. Heath, K. Shortman, and M. H. Lahoud. The dendritic cell subtype-restricted C-type lectin Clec9A is a target for vaccine enhancement. *Blood* 2008. 112: 3264–3273.
13. Chatterjee, B., A. Smed-Sorensen, L. Cohn, C. Chalouni, R. Vandlen, B.-C. Lee, J. Widger, T. Keler, L. Delamarre, and I. Mellman. Internalization and endosomal degradation of receptor-bound antigens regulate the efficiency of cross presentation by human dendritic cells. *Blood* 2012. 120: 2011–2020.
14. Singh, S. K., J. Stephani, M. Schaefer, H. Kalay, J. J. García-Vallejo, J. den Haan, E. Saeland, T. Sparwasser, and Y. van Kooyk. Targeting glycan modified OVA to murine DC-SIGN transgenic dendritic cells enhances MHC class I and II presentation. *Mol. Immunol.* 2009. 47: 164–174.
15. García-Vallejo, J. J., M. Ambrosini, A. Overbeek, W. E. van Riel, K. Bloem, W. W. J. Unger, F. Chiodo, J. G. Bolscher, K. Nazmi, H. Kalay, and Y. van Kooyk. Multivalent glycopeptide dendrimers for the targeted delivery of antigens to dendritic cells. *Mol. Immunol.* 2013. 53: 387–397.
16. Unger, W. W. J., A. J. Van Beelen, S. C. Bruijns, M. Joshi, C. M. Fehres, L. Van Bloois, M. I. Verstege, M. Ambrosini, H. Kalay, K. Nazmi, J. G. Bolscher, E. Hooijberg, T. D. De Gruijl, G. Storm, and Y. Van Kooyk. Glycan-modified liposomes boost CD4 + and CD8 + T-cell responses by targeting DC-SIGN on dendritic cells. *J. Control. Release* 2012. 160: 88–95.
17. Unger, W. W., C. T. Mayer, S. Engels, C. Hesse, M. Perdicchio, F. Puttur, I. Streng-Ouwehand, M. Litjens, H. Kalay, L. Berod, T. Sparwasser, and Y. van Kooyk. Antigen targeting to dendritic cells combined with transient regulatory T cell inhibition results in long-term tumor regression. *Oncoimmunology* 2015. 4: e970462.
18. Aarnoudse, C. A., M. Bax, M. Sánchez-Hernández, J. J. García-Vallejo, and Y. van Kooyk. Glycan modification of the tumor antigen gp100 targets DC-SIGN to enhance dendritic cell induced antigen presentation to T cells. *Int. J. cancer* 2008. 122: 839–846.

19. Yang, L., H. Yang, K. Rideout, T. Cho, K. Il Joo, L. Ziegler, A. Elliot, A. Walls, D. Yu, D. Baltimore, and P. Wang. Engineered lentivector targeting of dendritic cells for in vivo immunization. *Nat. Biotechnol.* 2008. 26: 326–334.
20. Singh, S. K., I. Streng-Ouwehand, M. Litjens, H. Kalay, S. Burgdorf, E. Saeland, C. Kurts, W. W. Unger, and Y. van Kooyk. Design of neo-glycoconjugates that target the mannose receptor and enhance TLR-independent cross-presentation and Th1 polarization. *Eur. J. Immunol.* 2011. 41: 916–925.
21. Burgdorf, S., C. Schölz, A. Kautz, R. Tampé, and C. Kurts. Spatial and mechanistic separation of cross-presentation and endogenous antigen presentation. *Nat. Immunol.* 2008. 9: 558–566.
22. Burgdorf, S., A. Kautz, V. Böhnert, P. A. Knolle, and C. Kurts. Distinct pathways of antigen uptake and intracellular routing in CD4 and CD8 T cell activation. *Science* 2007. 316: 612–616.
23. Taylor, M. E., K. Bezouska, and K. Drickamer. Contribution to ligand binding by multiple carbohydrate-recognition domains in the macrophage mannose receptor. *J. Biol. Chem.* 1992. 267: 1719–1726.
24. Singh, S. K., I. Streng-Ouwehand, M. Litjens, D. R. Weelij, J. J. García-Vallejo, S. J. van Vliet, E. Saeland, and Y. van Kooyk. Characterization of murine MGL1 and MGL2 C-type lectins: Distinct glycan specificities and tumor binding properties. *Mol. Immunol.* 2009. 46: 1249–1249.
25. Dupasquier, M., P. Stoitzner, H. Wan, D. Cerqueira, A. Van Oudenaren, J. S. A. Voerman, K. Denda-Nagai, T. Irimura, G. Raes, N. Romani, and P. J. M. Leenen. The dermal microenvironment induces the expression of the alternative activation marker CD301/mMGL in mononuclear phagocytes, independent of IL-4/IL-13 signaling. *J. Leukoc. Biol.* 2006. 80: 838–849.
26. Tsuiji, M., M. Fujimori, Y. Ohashi, N. Higashi, T. M. Onami, S. M. Hedrick, and T. Irimura. Molecular cloning and characterization of a novel mouse macrophage C-type lectin, mMGL2, which has a distinct carbohydrate specificity from mMGL1. *J. Biol. Chem.* 2002. 277: 28892–28901.
27. Denda-Nagai, K., S. Aida, K. Saba, K. Suzuki, S. Moriyama, S. Oo-puthinan, M. Tsuiji, A. Morikawa, Y. Kumamoto, D. Sugiura, A. Kudo, Y. Akimoto, H. Kawakami, N. V. Bovin, and T. Irimura. Distribution and function of macrophage galactose-type C-type lectin 2 (MGL2/CD301b): Efficient uptake and presentation of glycosylated antigens by dendritic cells. *J. Biol. Chem.* 2010. 285: 19193–19204.
28. Segura, E., E. Kapp, N. Gupta, J. Wong, J. Lim, H. Ji, W. R. Heath, R. Simpson, and J. A. Villadangos. Differential expression of pathogen-recognition molecules between dendritic cell subsets revealed by plasma membrane proteomic analysis. *Mol. Immunol.* 2010. 47: 1765–1773.
29. van Vliet, S. J., E. Saeland, and Y. van Kooyk. Sweet preferences of MGL: carbohydrate specificity and function. *Trends Immunol.* 2008. 29: 83–90.
30. van Vliet, S. J., C. A. Aarnoudse, V. C. M. Broks-van den Nerg, M. Boks, T. B. H. Geijtenbeek, and Y. van Kooyk. MGL-mediated internalization and antigen presentation by dendritic cells: A role for tyrosine-5. *Eur. J. Immunol.* 2007. 37: 2075–2081.
31. Yuita, H., M. Tsuiji, Y. Tajika, Y. Matsumoto, K. Hirano, N. Suzuki, and T. Irimura. Retardation of removal of radiation-induced apoptotic cells in developing neural tubes in macrophage galactose-type C-type lectin-1-deficient mouse embryos. *Glycobiology* 2005. 15: 1368–1375.
32. Gringhuis, S. I., T. M. Kaptein, B. A. Wevers, M. Van Der Vlist, E. J. Klaver, I. Van Die, L. E. M. Vriend, M. A. W. P. De Jong, and T. B. H. Geijtenbeek. Fucose-based PAMPs prime dendritic cells for follicular T helper cell polarization via DC-SIGN-dependent IL-27 production. *Nat. Commun.* 2014. 5: 5074.
33. Taylor, M. E., and K. Drickamer. Structural requirements for high affinity binding of complex ligands by the macrophage mannose receptor. *J. Biol. Chem.* 1993. 268: 399–404.
34. Burgdorf, S., V. Lukacs-Kornek, and C. Kurts. The mannose receptor mediates uptake of soluble but not of cell-associated antigen for cross-presentation. *J. Immunol.* 2006. 176: 6770–6776.
35. Gervais, F., M. Stevenson, and E. Skamene. Genetic control of resistance to *Listeria monocytogenes*: regulation of leukocyte inflammatory responses by the Hc locus. *J. Immunol.* 1984. 132: 2078–83.
36. Hsieh, C. S., S. E. Macatonia, A. O'Garra, and K. M. Murphy. T cell genetic background determines default t helper phenotype development in vitro. *J. Exp. Med.* 1995. 181: 713–721.
37. Blander, J. M., and R. Medzhitov. On regulation of phagosome maturation and antigen presentation. *Nat. Immunol.* 2006. 7: 1029–1035.
38. Amigorena, S., and A. Savina. Intracellular mechanisms of antigen cross presentation in dendritic cells. *Curr. Opin. Immunol.* 2010. 22: 109–117.
39. Adiko, A. C., J. Babbor, E. Gutiérrez-Martínez, P. Guermonprez, and L. Saveanu. Intracellular transport routes for MHC I and their relevance for antigen cross-presentation. *Front. Immunol.* 2015. 6: 335.

40. Shen, L., L. J. Sigal, M. Boes, and K. L. Rock. Important role of cathepsin S in generating peptides for TAP-independent MHC class I crosspresentation in vivo. *Immunity* 2004. 21: 155–165.
41. Nakagawa, T. Y., W. H. Brissette, P. D. Lira, R. J. Griffiths, N. Petrushova, J. Stock, J. D. McNeish, S. E. Eastman, E. D. Howard, S. R. Clarke, E. F. Rosloniec, E. A. Elliott, and A. Y. Rudensky. Impaired invariant chain degradation and antigen presentation and diminished collagen-induced arthritis in cathepsin S null mice. *Immunity* 1999. 10: 207–217.
42. Van Montfoort, N., M. G. Camps, S. Khan, D. V. Filippov, J. J. Weterings, J. M. Griffith, H. J. Geuze, T. van Hall, J. S. Verbeek, C. J. Melief, and F. Ossendorp. Antigen storage compartments in mature dendritic cells facilitate prolonged cytotoxic T lymphocyte cross-priming capacity. *Proc. Natl. Acad. Sci. U. S. A.* 2009. 106: 6730–6735.
43. Kovacovics-Bankowski, M., and K. L. Rock. A phagosome-to-cytosol pathway for exogenous antigens presented on MHC class I molecules. *Science* 1995. 267: 243–246.
44. Sancho, D., D. Mourão-Sá, O. P. Joffre, O. Schulz, N. C. Rogers, D. J. Pennington, J. R. Carlyle, and C. R. Sousa. Tumor therapy in mice via antigen targeting to a novel, DC-restricted C-type lectin. *J. Clin. Invest.* 2008. 118: 2098–2110.
45. Segura, E., A. L. Albiston, I. P. Wicks, S. Y. Chai, and J. A. Villadangos. Different cross-presentation pathways in steady-state and inflammatory dendritic cells. *Proc. Natl. Acad. Sci. U. S. A.* 2009. 106: 20377–20381.
46. Sancho, D., O. P. Joffre, A. M. Keller, N. C. Rogers, D. Martínez, P. Hernanz-Falcón, I. Rosewell, and C. R. E. Sousa. Identification of a dendritic cell receptor that couples sensing of necrosis to immunity. *Nature* 2009. 458: 899–903.
47. Li, D., G. Romain, A.-L. Flamar, D. Duluc, M. Dullaers, X.-H. Li, S. Zurawski, N. Bosquet, A. K. Palucka, R. Le Grand, A. O'Garra, G. Zurawski, J. Banchereau, and S. Oh. Targeting self- and foreign antigens to dendritic cells via DC-ASGPR generates IL-10-producing suppressive CD4+ T cells. *J. Exp. Med.* 2012. 209: 109–121.
48. van Vliet, S. J., S. Bay, I. M. Vuist, H. Kalay, J. J. García-Vallejo, C. Leclerc, and Y. van Kooyk. MGL signaling augments TLR2-mediated responses for enhanced IL-10 and TNF- α secretion. *J. Leukoc. Biol.* 2013. 94: 315–323.
49. Saba, K., K. Denda-Nagai, and T. Irimura. A C-type lectin MGL1/CD301a plays an anti-inflammatory role in murine experimental colitis. *Am. J. Pathol.* 2009. 174: 144–152.
50. Westcott, D. J., J. B. Delproposito, L. M. Geletka, T. Wang, K. Singer, A. R. Saltiel, and C. N. Lumeng. MGL1 promotes adipose tissue inflammation and insulin resistance by regulating 7/4hi monocytes in obesity. *J. Exp. Med.* 2009. 206: 3143–3156.
51. Guermónprez, P., L. Saveanu, M. Kleijmeer, J. Davoust, P. Van Endert, and S. Amigorena. ER-phagosome fusion defines an MHC class I cross-presentation compartment in dendritic cells. *Nature* 2003. 425: 397–402.
52. Houde, M., S. Bertholet, E. Gagnon, S. Brunet, G. Goyette, A. Laplante, M. F. Princiotto, P. Thibault, D. Sacks, and M. Desjardins. Phagosomes are competent organelles for antigen cross-presentation. *Nature* 2003. 425: 402–406.
53. Burgdorf, S., and C. Kurts. Endocytosis mechanisms and the cell biology of antigen presentation. *Curr. Opin. Immunol.* 2008. 20: 89–95.
54. Mintern, J. D., C. Macri, and J. A. Villadangos. Modulation of antigen presentation by intracellular trafficking. *Curr. Opin. Immunol.* 2015. 34: 16–21.
55. Nair-Gupta, P., A. Baccharini, N. Tung, F. Seyffer, O. Florey, Y. Huang, M. Banerjee, M. Overholtzer, P. A. Roche, R. Tampé, B. D. Brown, D. Amsen, S. W. Whiteheart, and J. M. Blander. TLR signals induce phagosomal MHC-I delivery from the endosomal recycling compartment to allow cross-presentation. *Cell* 2014. 158: 506–521.
56. Cebrian, I., G. Visentin, N. Blanchard, M. Jouve, A. Bobard, C. Moita, J. Enninga, L. F. Moita, S. Amigorena, and A. Savina. Sec22b regulates phagosomal maturation and antigen crosspresentation by dendritic cells. *Cell* 2011. 147: 1355–1368.
57. Lieberoth, A., F. Splittstoesser, N. Katagihallimath, I. Jakovcevski, G. Loers, B. Ranscht, D. Karageorgos, M. Schachner, and R. Kleene. Lewis x and α 2,3-sialyl glycans and their receptors TAG-1, contactin, and L1 mediate CD24-dependent neurite outgrowth. *J. Neurosci.* 2009. 29: 6677–6690.
58. Read, T.-A., M. P. Fogarty, S. L. Markant, R. E. McLendon, Z. Wei, D. W. Ellison, P. G. Febbo, and R. J. Wechsler-Reya. Identification of CD15 as a marker for tumor-propagating cells in a mouse model of medulloblastoma. *Cancer Cell* 2009. 15: 135–147.

Chapter 5

59. Hittelet, A., I. Camby, N. Nagy, H. Legendre, Y. Bronckart, C. Decaestecker, H. Kaltner, N. E. Nifant'ev, N. V. Bovin, J.-C. Pector, I. Salmon, H.-J. Gabius, R. Kiss, and P. Yeaton. Binding sites for Lewis antigens are expressed by human colon cancer cells and negatively affect their migration. *Lab. Invest.* 2003. 83: 777–87.
60. Ohana-Malka, O., D. Benharroch, N. Isakov, I. Prinsloo, G. Shubinsky, M. Sacks, and J. Gopas. Selectins and anti-CD15 (Lewis x/a) antibodies transmit activation signals in Hodgkin's lymphoma-derived cell lines. *Exp. Hematol.* 2003. 31: 1057–1065.
61. Bergman, M. P., A. Engering, H. H. Smits, S. J. Van Vliet, A. A. Van Bodegraven, H. P. Wirth, M. L. Kapsenberg, C. M. J. E. Vandenbroucke-Grauls, Y. Van Kooyk, and B. J. Appelmelk. Helicobacter pylori modulates the T helper cell 1/T helper cell 2 balance through phase-variable interaction between lipopolysaccharide and DC-SIGN. *J. Exp. Med.* 2004. 200: 979–990.
62. Saeland, E., and Y. Van Kooyk. Highly glycosylated tumour antigens: Interactions with the immune system. *Biochem. Soc. Trans.* 2011. 39: 388–392.
63. Kalay, H., M. Ambrosini, P. H. C. Van Berkel, P. W. H. I. Parren, Y. Van Kooyk, and J. J. García Vallejo. Online nanoliquid chromatography-mass spectrometry and nanofluorescence detection for high-resolution quantitative N-glycan analysis. *Anal. Biochem.* 2012. 423: 153–162.

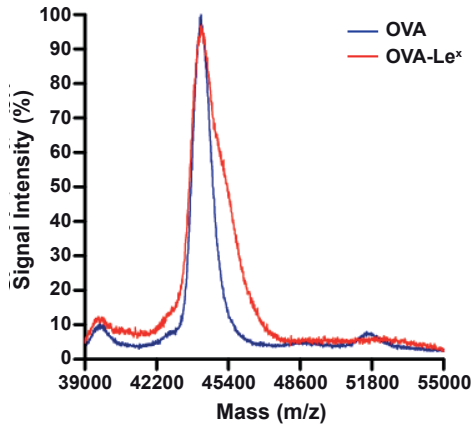


Figure 1-figure supplement 1. The MALDI-TOF/TOF mass spectrum of OVA-Le^x (Red) shows an increase of 1,2 KDa compared to unconjugated OVA (Blue), corresponding to addition of two Le^x molecules per OVA molecule.

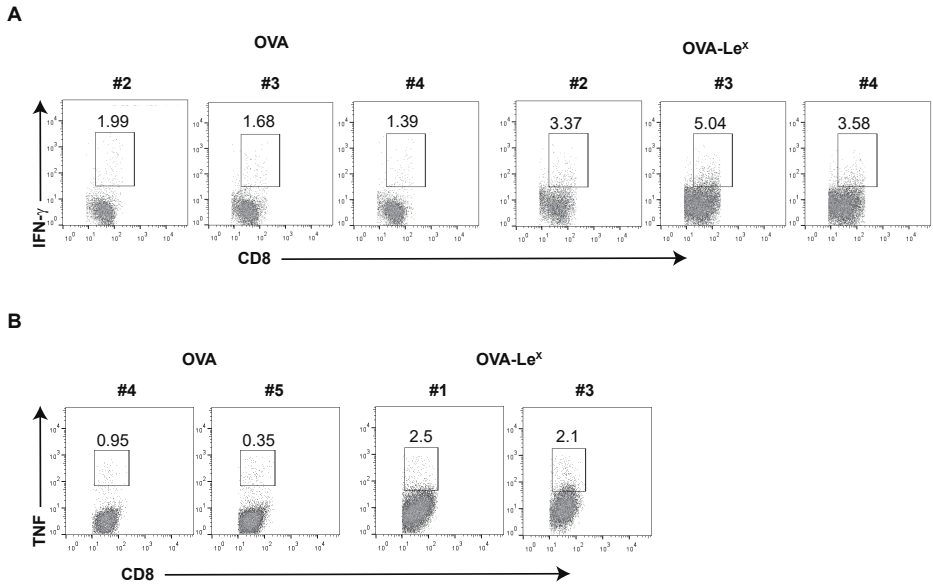


Figure 2-figure supplement 1. Representative flow cytometry plots of (A) IFN- γ and (B) TNF- producing CD8⁺ T cells in spleens of C57BL/6 mice that were immunized with either OVA-Le^x or native OVA mixed with anti-CD40 using a prime-boost protocol; numbers above the gates designate the percentage of IFN- γ ⁺ or TNF⁺ CD8⁺ T cells.

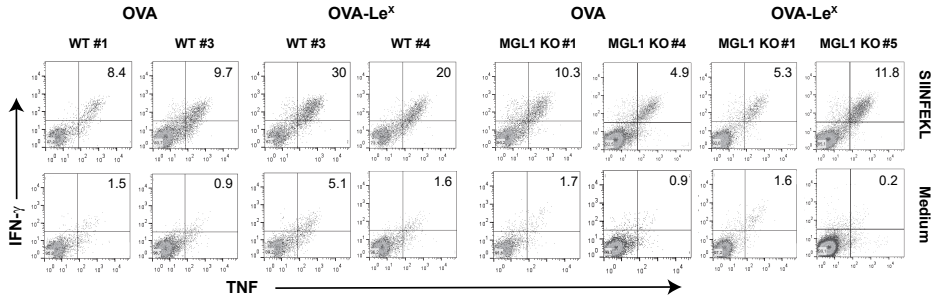


Figure 2-figure supplement 2. C57BL/6 and MGL1 KO mice were prime-boosted with either OVA-Le^x or native OVA mixed with anti-CD40. Frequencies of IFN- γ and TNF-double-producing CD8⁺ T cells were determined by intracellular staining after re-stimulation of splenocytes *ex vivo*. Representative FACS plots of indicated mice are shown; numbers designate the percentage of IFN- γ and TNF-double positive CD8⁺ T cells.

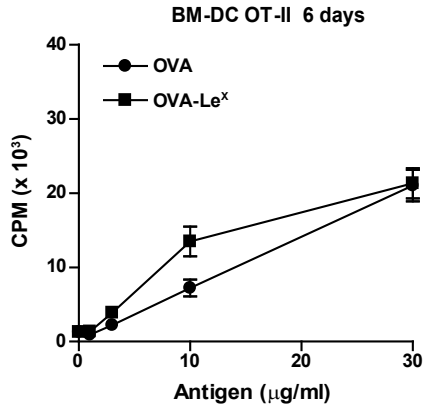


Figure 3-figure supplement 1. No enhanced expansion of OT-II T cells when co-cultured for six days with OVA-Le^x pulse-loaded DCs. WT BM-DCs were loaded with OVA-Le^x or native OVA for 4h and subsequently co-cultured with OT-II T cells for six days. Proliferation of OT-II T cells was determined by [³H]-thymidine uptake and presented as mean \pm SD of triplicate cultures. Data shown are representative of two independent experiments.

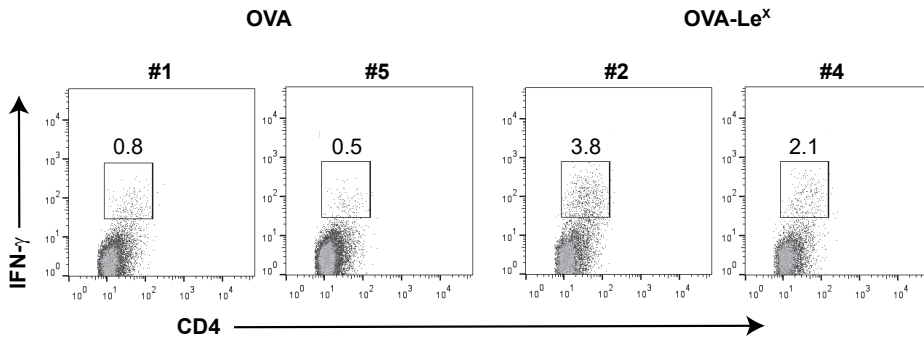


Figure 3-figure supplement 2. C57BL/6 mice were immunized s.c. with either OVA-Le^x or native OVA mixed with anti-CD40 using a prime-boost protocol and the frequency of IFN- γ -producing activated CD4⁺ T cells in spleen was determined by intracellular staining after OVA-specific re-stimulation *ex vivo*. Representative FACS plots of indicated mice are shown; numbers above the gates designate the percentage of IFN- γ CD4⁺ T cells.

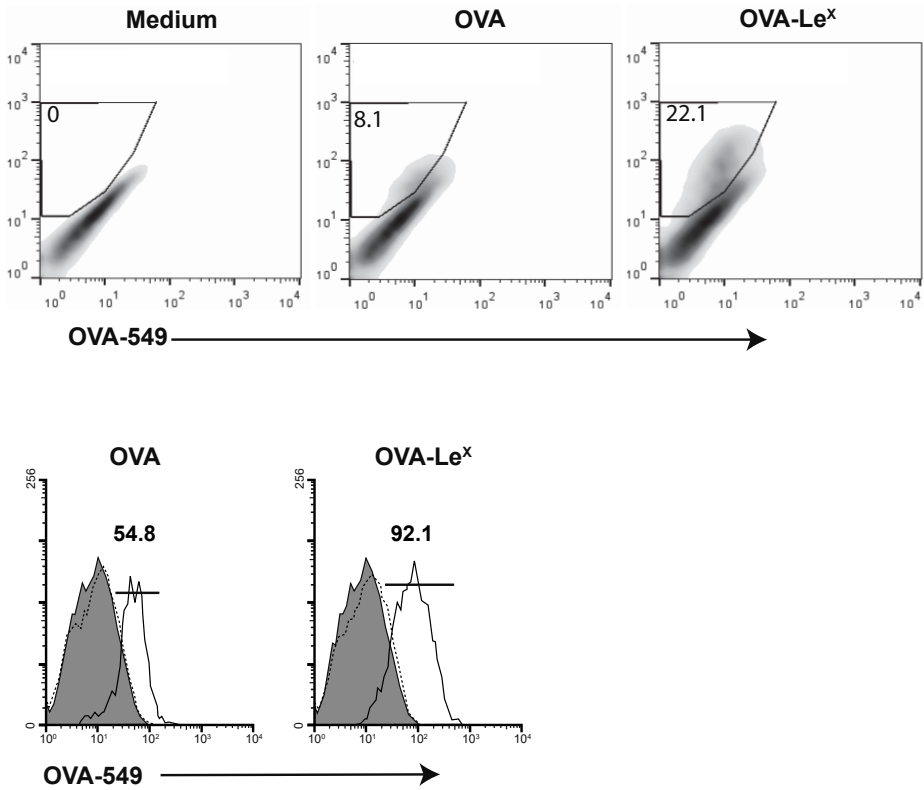


Figure 4-figure supplement 1. Uptake of fluorescent-labeled OVA-Le^x or native OVA (30 μ g/ml) by WT BM-DCs was analyzed by flow cytometry after 90 min (upper panel). Control cells were incubated with medium. The percentage of gated antigen- positive DCs are indicated. Lower panel: histograms indicating the mean uptake of OVA (left, black line) or OVA-Le^x (right, black line) versus medium (grey filled histograms) and EGTA (dashed lines) controls. Numbers indicate the MFI of OVA- positive DCs.

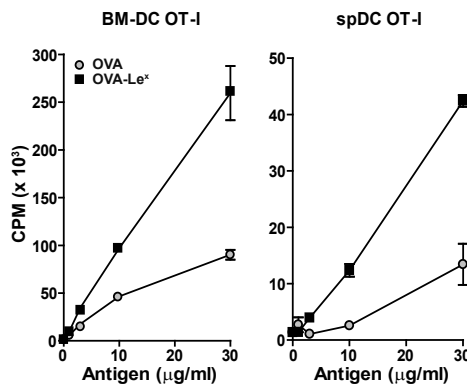


Figure 4-figure supplement 2. Enhanced cross-presentation of OVA-Le^x by DCs as measured by ³H-Thymidine incorporation. BM-DCs and CD11c⁺ spDCs loaded with OVA-Le^x enhanced OT-I proliferation compared to native OVA loaded DCs. Proliferation was determined on day 3 by [³H]-Thymidine uptake and presented as mean \pm SD of triplicate cultures. Data are representative of four independent experiments.

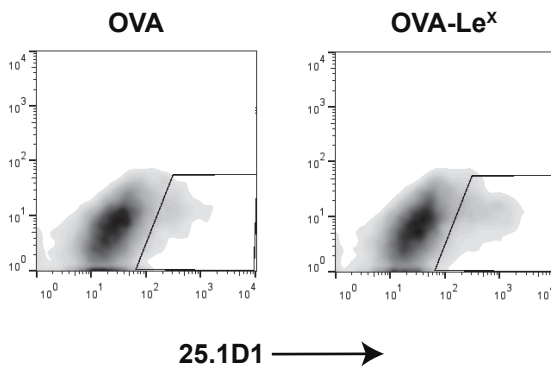


Figure 4-figure supplement 3. Representative flow cytometry plots of 25.1D1 staining of BM-DCs 18h after pulse loading with OVA-Le^x or native OVA (750 ug/ml).

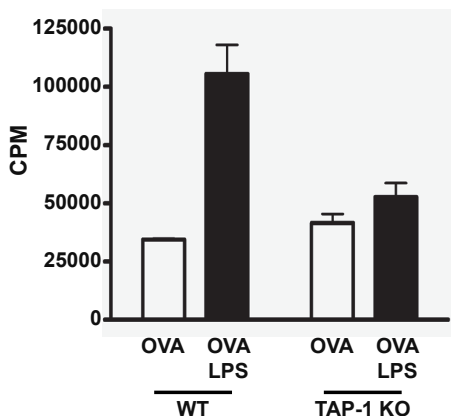


Figure 4-figure supplement 4. Cross-presentation of OVA requires TLR4 triggering and is TAP-dependent. WT or TAP-1-deficient BM-DCs were loaded with OVA (0.5 mg/ml) in the presence or absence of 100 ng/ml LPS and subsequently co-cultured with purified OT-I T cells for 3 days. [3H]-Thymidine is incorporated during the last 18h and is presented as mean±SD of triplicate cultures. Data are representative of two independent experiments.

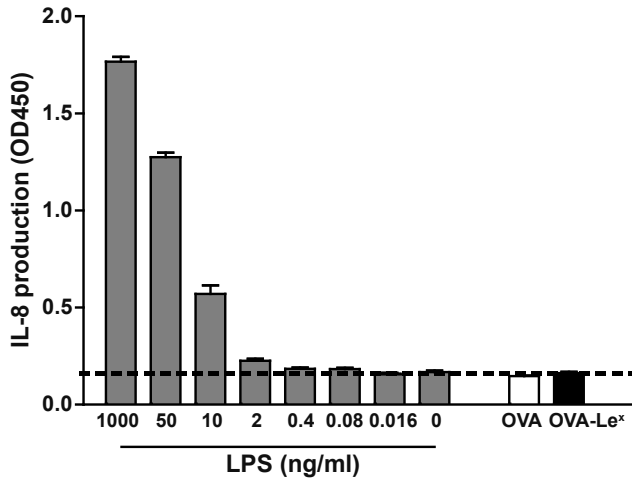


Figure 4-figure supplement 5. OVA-Le^x formulations are free of endotoxins. Both OVA and OVA-Le^x were tested for endotoxin levels. Human embryonic kidney (HEK)293-TLR4/MyD88 transfectants (kind gift of Dr. D. Golenbock) were cultured in the presence of either antigen preparation (30 µg/ml) or indicated amounts of *E. coli*-derived LPS (Sigma Aldrich). The HEK transfectants respond to LPS by secreting IL-8. In both preparations, LPS was below detection limits (dashed line). Results are representative of two independent experiments.

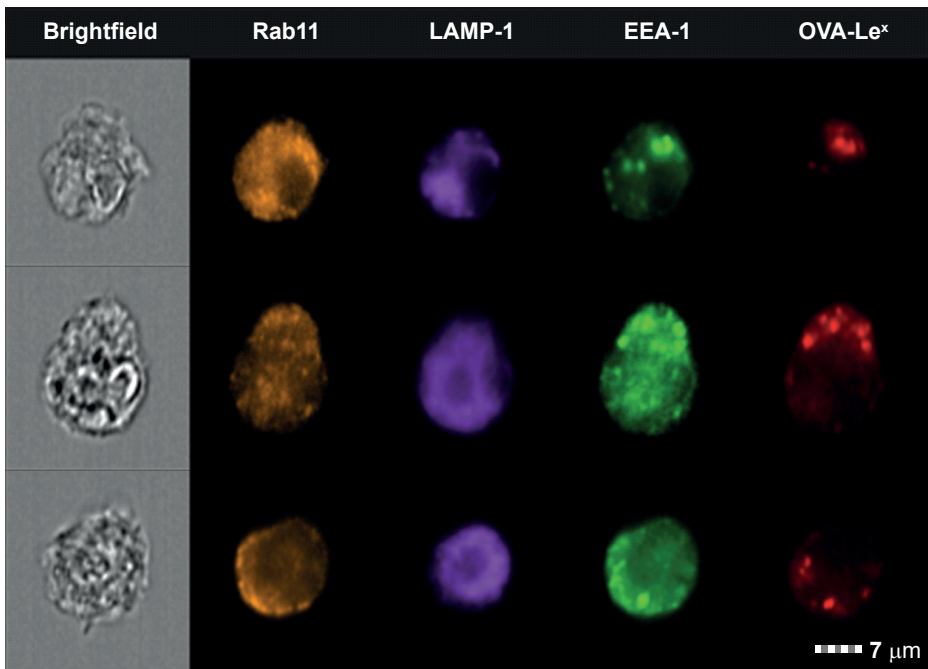


Figure 6-figure supplement 1. Examples of WT BM-DCs pulsed with Alexa Fluor 674-OVA-Le^x displaying high co-localization of OVA-Le^x with EEA-1 and Rab11 as measured by imaging flow cytometry.

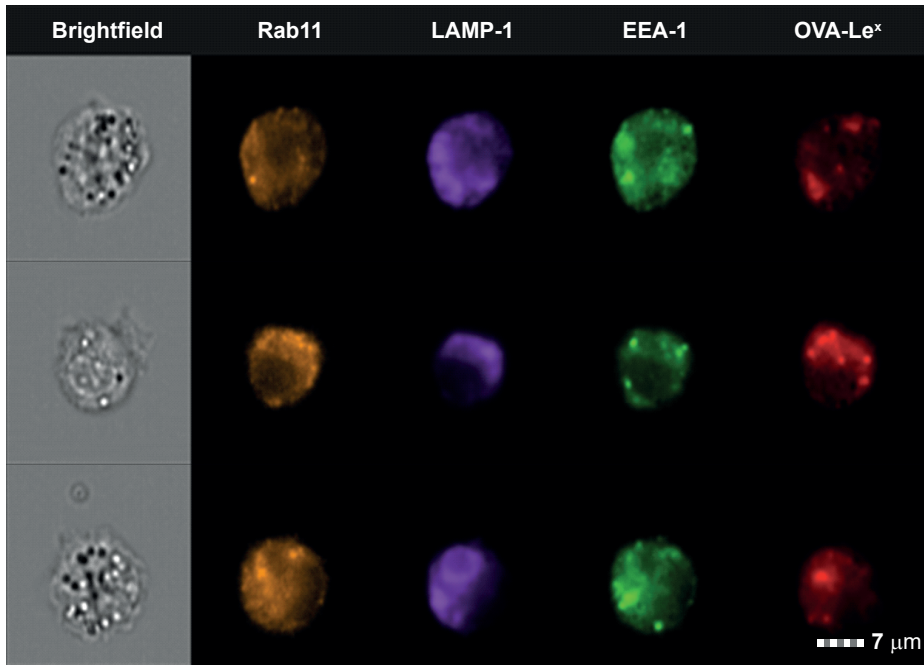


Figure 6-figure supplement 2. Examples of WT BM-DCs pulsed with Alexa Fluor 674-OVA-Le^x displaying high co-localization of OVA-Le^x with LAMP1 and Rab11 as measured by imaging flow cytometry.

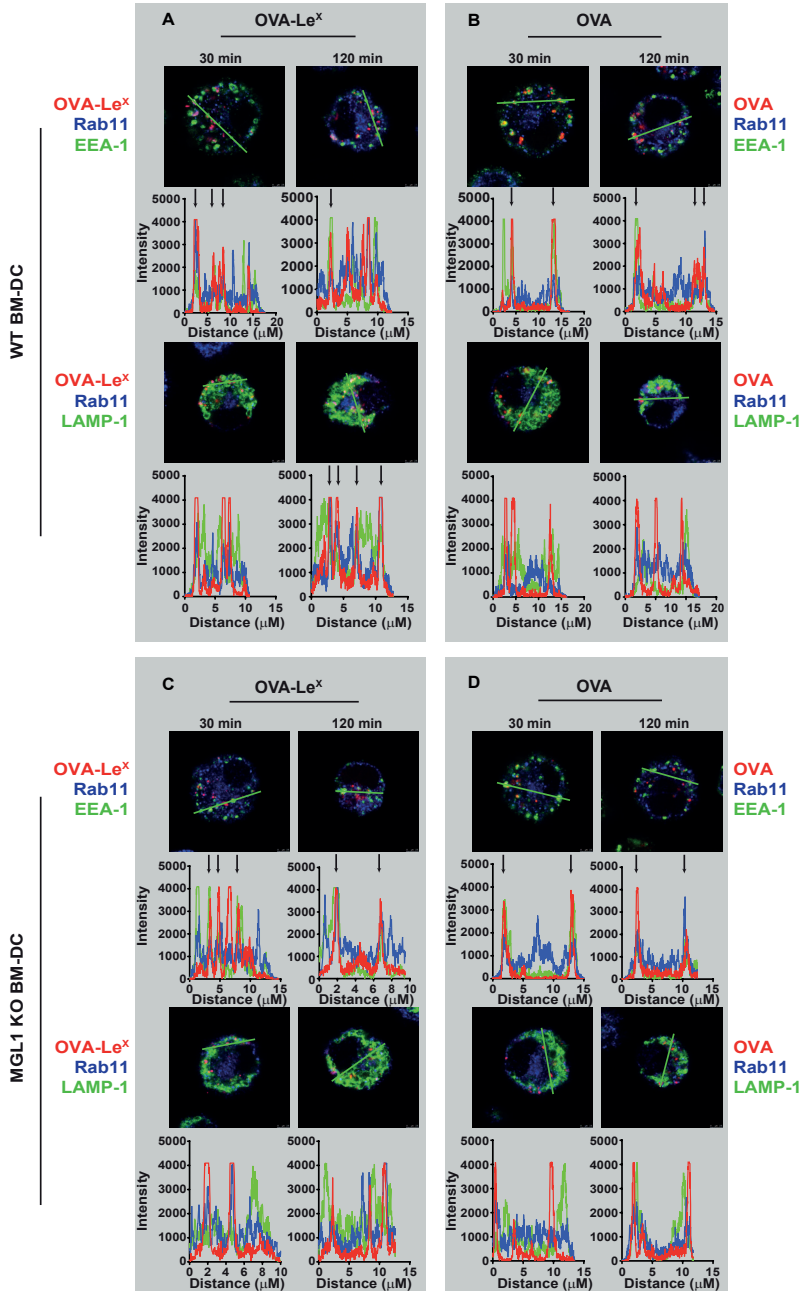


Figure 6-figure supplement 3. WT (upper panels) and MGL1 KO (lower panels) BM-DCs were incubated with Dylight-633-OVA-Le^x or native OVA (30 μg/ml) and 30min or 2h later co-localization of OVA antigen (Red) with early endosomal (EEA-1, Green) or endosomal/lysosomal (LAMP1, Green) and recycling endosomal (Rab11, Blue) compartments was analyzed using CSLM. From a z-stack, histograms were created for a selected area (indicated by a line) using the Leica confocal software. Histograms were created from each fluorochrome and overlays were made by the program. Arrows indicate co-localization of antigen (Red) with EEA1&Rab11 or LAMP1&Rab11.